

cy.2

JUL 29 1983

AUG 30 1988

OCT 11 1991



COMPUTERIZED HEAT-TRANSFER AND STRESS ANALYSIS OF WIND TUNNEL METAL THROAT LINERS

Dennis T. Akers

ARO, Inc., a Sverdrup Corporation Company

VON KÁRMÁN GAS DYNAMICS FACILITY
ARNOLD ENGINEERING DEVELOPMENT CENTER
AIR FORCE SYSTEMS COMMAND
ARNOLD AIR FORCE STATION, TENNESSEE 37389

November 1978

Final Report for Period June 2, 1977 — June 22, 1978

Approved for public release; distribution unlimited.

**TECHNICAL REPORTS
FILE COPY**

Property of U. S. Air Force
AEDC LIBRARY
F40600-27-C-0003

Prepared for

ARNOLD ENGINEERING DEVELOPMENT CENTER/DO
ARNOLD AIR FORCE STATION, TENNESSEE 37389

NOTICES

When U. S. Government drawings, specifications, or other data are used for any purpose other than a definitely related Government procurement operation, the Government thereby incurs no responsibility nor any obligation whatsoever, and the fact that the Government may have formulated, furnished, or in any way supplied the said drawings, specifications, or other data, is not to be regarded by implication or otherwise, or in any manner licensing the holder or any other person or corporation, or conveying any rights or permission to manufacture, use, or sell any patented invention that may in any way be related thereto.

Qualified users may obtain copies of this report from the Defense Documentation Center.

References to named commercial products in this report are not to be considered in any sense as an indorsement of the product by the United States Air Force or the Government.

This report has been reviewed by the Information Office (OI) and is releasable to the National Technical Information Service (NTIS). At NTIS, it will be available to the general public, including foreign nations.

APPROVAL STATEMENT

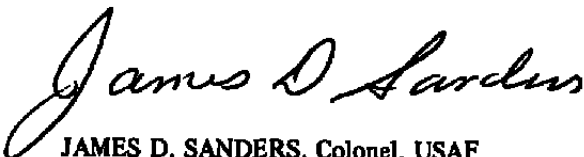
This report has been reviewed and approved.



ERVIN P. JASKOLSKI, Captain, USAF
Test Director, VKF Division
Directorate of Test Operations

Approved for publication:

FOR THE COMMANDER



JAMES D. SANDERS, Colonel, USAF
Director of Test Operations
Deputy for Operations

UNCLASSIFIED

20. ABSTRACT (Continued)

order to maintain liner configurations to produce accurate test conditions, the liners must be externally cooled, usually with water. In doing this, thermal gradients are set up in the liner and an analysis must be made to ensure adequate design. One of the most difficult problems in analyzing the liner is determining the airside, forced-convection, heat-transfer coefficient. The main reason it is so difficult is due to the boundary layer that develops along the contour of the liner. Sivells, ARO, Inc., derived, programmed, and experimentally checked a method for calculating the turbulent boundary-layer properties in the supersonic section of a liner. Using the results from Sivells' program and an iterative radial heat balance, one can write a subroutine, called HEAT, to determine the following: 1) The thermal gradient through the thickness of the liner; 2) The temperature profile along the length of the liner; and 3) The total stresses at any point in the liner. Included in the subroutine is a method for determining the same three conditions for the subsonic section of the liner. This gives a complete analysis of the entire liner. Thus, the design analysis of a wind tunnel liner, both aerodynamically and structurally, can be performed using one program. The program will also solve any number of cases at one time. An example problem is presented showing all steps required to operate the program.

PREFACE

The work reported herein was conducted by the Arnold Engineering Development Center (AEDC), Air Force Systems Command (AFSC) under Program Element 65807F. The results were obtained by ARO, Inc. (a Sverdrup Corporation Company), contract operator for AEDC, AFSC, under ARO Project No. V44A. The manuscript was submitted for publication on August 10, 1978.

The report of this work was submitted by the author in partial fulfillment of the requirements for a Master of Science degree from The University of Tennessee, Knoxville, Tennessee, in June 1978.

The author wishes to express appreciation to Dr. Firouz Shahrokhi; University of Tennessee Space Institute, Tullahoma, Tennessee, for his advice and encouragement throughout this study. Appreciation is especially due Gerald Gillis, ARO, Inc. for scheduling the author's work assignments to allow completion of this work.

TABLE OF CONTENTS

CHAPTER	PAGE
I. INTRODUCTION	5
II. SUPERSONIC HEAT-TRANSFER ANALYSIS	10
III. SUBSONIC HEAT-TRANSFER ANALYSIS	25
IV. STRESS ANALYSIS	28
Thermal Stresses	28
Subsonic Pressure Stresses	29
Supersonic Pressure Stresses	31
Total Stresses	31
V. SUMMARY AND RECOMMENDATIONS	33
VI. HEAT SUBROUTINE	36
Block Diagram	36
HEAT Listing	39
VII. INSTRUCTIONS FOR HEAT USERS	46
Subroutine Function	46
Input Data	46
VIII. EXAMPLE PROBLEM	51
BIBLIOGRAPHY	64

APPENDIXES

APPENDIX A. EQUATION DEVELOPMENT FOR SMOOTH SUBSONIC CONTOURS	66
APPENDIX B. AXIAL FORCE EQUATION DEVELOPMENT	78

LIST OF FIGURES

FIGURE	PAGE
1. Typical Liner Assembly	7
2. Liner Throat Section Showing Heat Flow	11
3. Characteristic Diagram for Inviscid Supersonic Contour.	14
4. Example Problem Results.	63
5. Continuous Smooth Curvature for Liner Subsonic Section	67
6. Liner Segment Showing Load Distribution for Subsonic Section	79
7. Liner Segment Showing Load Distribution for Supersonic Section	80
NOMENCLATURE	83

CHAPTER I INTRODUCTION

Wind tunnels are used to simulate altitude conditions for testing of models of flight vehicles. The heart of the wind tunnel is the converging-diverging nozzle or liner. The liner shape provides the means of obtaining the desired properties of the flowing medium, usually air. Thus, its contour accuracy dictates the accuracy of the tunnel test conditions.

High air temperatures needed for model heat-transfer studies have required external cooling of the liners to keep their contour and thereby tunnel test conditions constant. The cooling is also needed to maintain structural strength. However, this cooling requirement induces thermal stresses in the liner that are usually significant compared to air- and cooling water-pressure stresses. Thus, the thermal stresses are generally a design basis. Since the region at the throat is usually the hottest, the throat calculation is the most critical and needs to be as accurate as possible. Therefore, an accurate heat-transfer analysis is needed to design an adequate liner.

At Arnold Engineering Development Center (AEDC), continuous-flow, axisymmetric, supersonic wind tunnels are in common use. Thus, a means of analyzing liners as accurately and quickly as possible is needed.

A typical axisymmetric throat assembly used at the von Karman Facility (VKF) of AEDC is shown in Fig. 1. The downstream flange is bolted to the shell assembly. The upstream flange has radial supports but is free to move axially. This allows for axial thermal growth due to temperature increase of the throat liner material. The thin cooling-water channel can be seen along the outside contour of the liner.

Because of the dependence of air and water properties on temperature, heat-transfer analysis of this type of liner is very difficult, generally requiring tedious iterative solutions. The high-speed digital computer has helped solve that part of the problem. The difficult problem is to determine accurately the heat transfer across the boundary layer that forms along the inside liner contour.

At AEDC, Sivells [1, 2, 3]¹ developed, programmed, and experimentally checked a method of calculating the supersonic boundary-layer properties for liners. This investigation uses the results of Sivells' program to perform a heat-transfer analysis for the liner shown in Fig. 1. Since Sivells' program calculates only the supersonic boundary-layer properties, the subsonic airside heat-transfer coefficient was estimated by an equation

¹Numbers in brackets refer to similarly numbered references in the Bibliography.

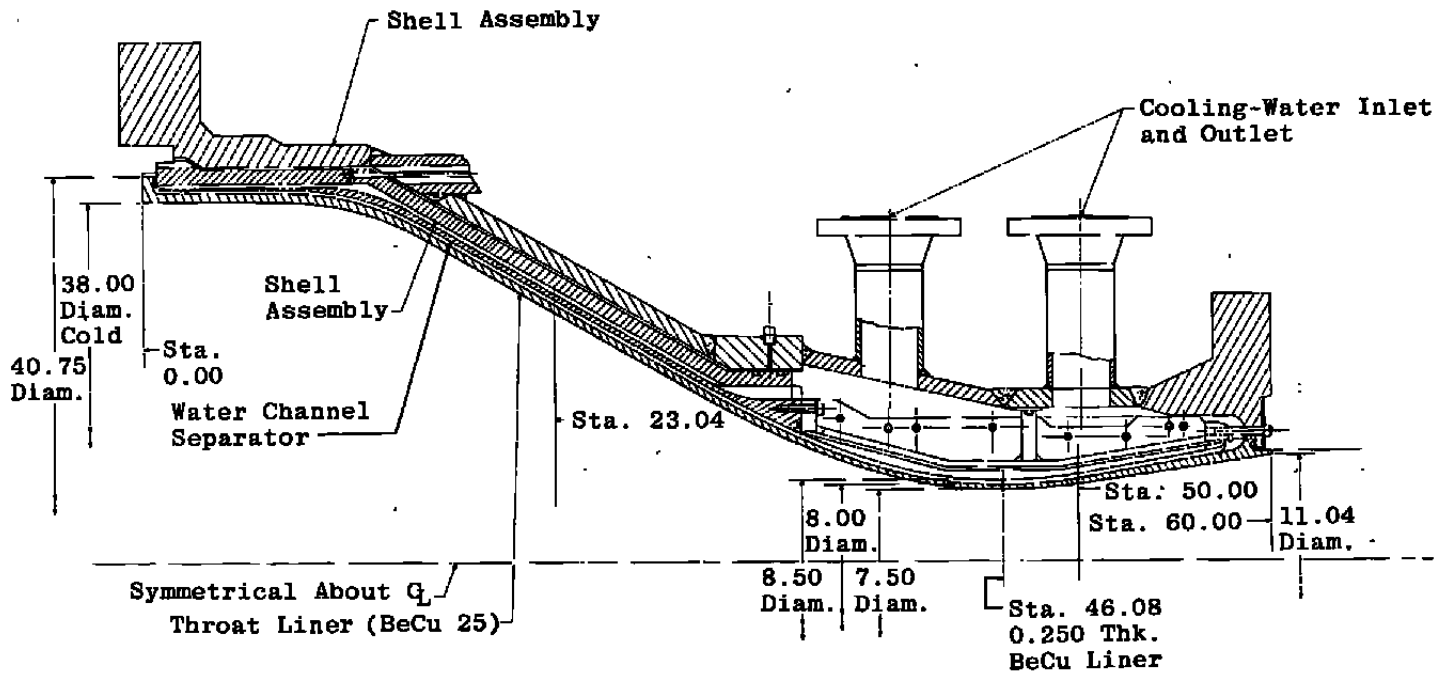


Figure 1. Typical liner assembly.

from Bartz [4, 5]; then a subsonic heat-transfer analysis was made.

Once the radial temperature distribution throughout the liner was known, a stress analysis was possible. Thermal, air-pressure, and water-pressure stresses were calculated, combined where applicable, and then maximums were found by applying a theory of failure.

Although restrictive thermal stresses are usually higher near the throat, the thermal stress near the ends should also be determined so that a combined thermal, pressure, and support stress can be checked. Also, the thermal stresses at the ends could be unpredictable because the liner is larger on the ends making the cooling-water velocity less, and the liner is usually thicker for adequate supporting. Since support of the ends of the liners is not always the same, support stresses were not included in this analysis. Thus, the subroutine in this study was written so that any point along the liner could be analyzed for thermal and pressure stresses.

The result is a subroutine, HEAT, that can be added to a boundary-layer program to perform a complete design analysis; this enables a much faster and more accurate analysis to be made. Also, the liner can be optimized by looking at many variations of parameters. Heretofore, the aerodynamic design was made and the results were sent to the structural analysis section for analysis.

Now, main structural and aerodynamic analysis can be made at one time.

CHAPTER II SUPERSONIC HEAT-TRANSFER ANALYSIS

The heat-transfer analysis of a wind tunnel metal throat liner, especially in the supersonic region where model test conditions are established, requires a careful consideration of the boundary-layer effect on the airside heat-transfer coefficient. The boundary layer is a thin film of the flowing medium in which a pronounced velocity and temperature gradient exist. The velocity varies from the free stream velocity on the medium side to zero at the wall. The temperature varies from the free stream to an adiabatic wall temperature. This boundary layer is turbulent over the entire length of the liner and its effects are discussed as follows.

Figure 2 shows a cross section of a liner assembly at its minimum flow area, the throat. The hot medium, usually air, flows through the liner and transmits heat to the inside surface by forced convection. The heat transferred can be calculated by Newton's law of cooling [6]. Thus, the heat rate equation is

$$q_a = h_a A_a (T_r - T_a) . \quad (1)$$

The area, A_a , is the inside surface of the liner that the air flows past. It is the inside circumference, c ,

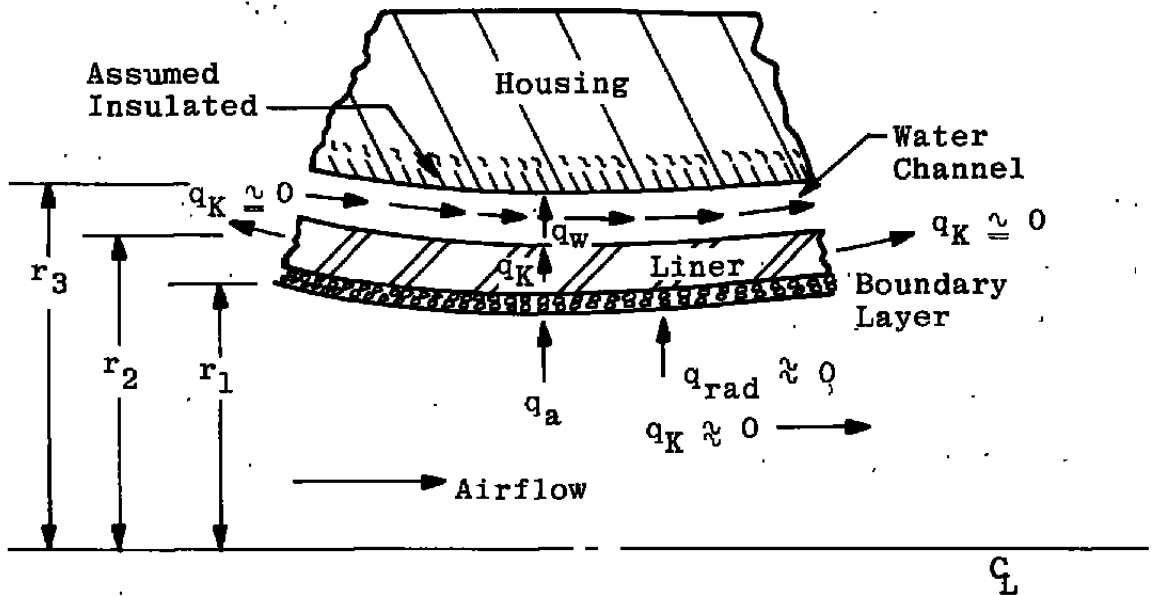


Figure 2. Liner throat section showing heat flow.

times a length, L . Since the axial thermal gradient is relatively small and the length is not used in the actual solution of the problem, as will be seen later, an incremental length, ΔL , may be substituted for L .

The recovery temperature, T_r , is the temperature of the inside liner surface based on an efficiency of the boundary layer to transmit the heat from the air to the wall. The recovery temperature is defined by Eckert [7] as

$$T_r = T_\infty + r (T_0 - T_\infty) , \quad (2)$$

where T_∞ is the static temperature and T_0 is the stagnation temperature of the air stream. The recovery factor, r , was assumed to be constant at 0.87.

The airside heat-transfer coefficient, h_a , was calculated by Reynolds analogy [6]. The equation is

$$St Pr^{2/3} = \frac{CF}{2} , \quad (3)$$

where

$$St = \frac{h_a}{\rho Cp u} . \quad (4)$$

Substitution of Eq. (4) into Eq. (3) yields an equation for the airside heat-transfer coefficient, h_a , which is

$$h_a = \frac{\rho Cp u (CF) (Pr)^{-2/3}}{2} . \quad (5)$$

The density, ρ , specific heat, C_p , and Prandtl number, Pr , for air are determined at a reference temperature defined as [6]

$$T_P = T_\infty + 0.5 (T_a - T_\infty) + 0.22 (T_r - T_\infty) . \quad (6)$$

This temperature corrects the constant-property, heat-transfer equations for the change in properties due to a temperature gradient across the boundary layer.

The skin-friction coefficient, CF , was determined by a method described by Sivells [1]. It was programmed for a 370/165 IBM computer. The method requires an iteration procedure and is explained as follows.

Briefly, Sivells' program calculates the skin-friction coefficient and the inviscid nozzle contour by an improved version of the method of characteristics described in [1] and illustrated in Fig. 3. Transonic theory determines a right-running characteristic TI , from the inviscid throat point. The axial velocity distribution between the upstream end, I , and downstream end, E , is described by a cubic equation which matches the velocity and first and second derivatives of velocity with the transonic values at I , and radial flow values at E . Between the left- and right-running characteristics through the inflection point, A , the flow is assumed to be radial. Between points B and C , the axial Mach number distribution is described by a fourth-degree polynomial. The point C is

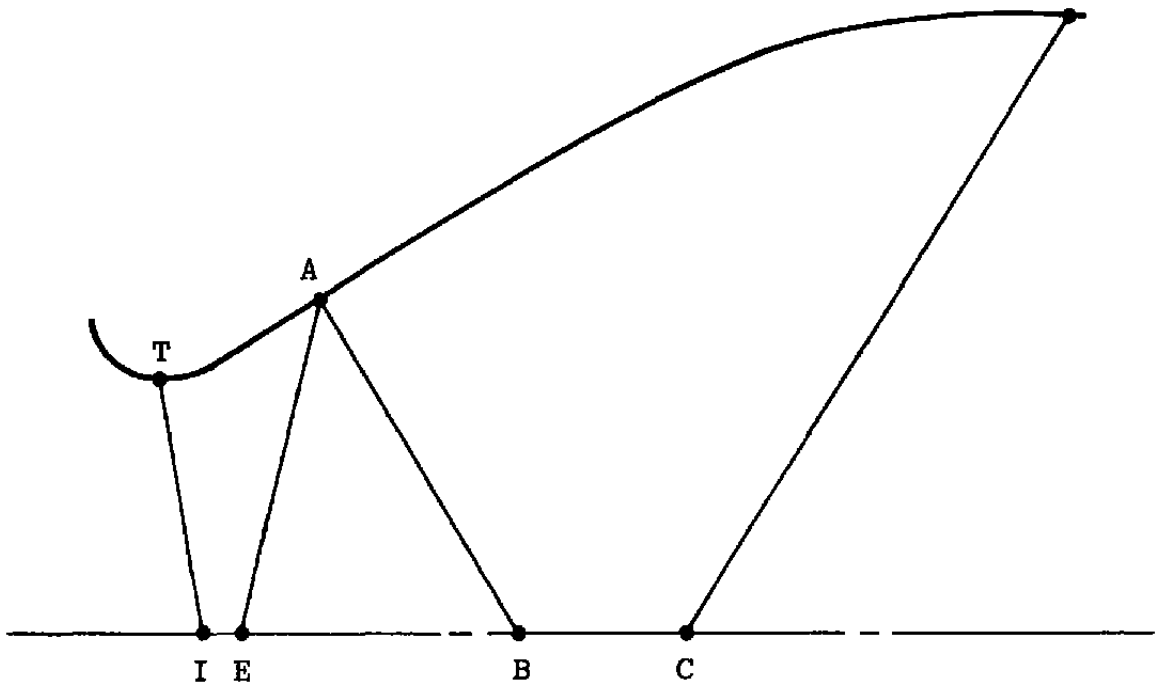


Figure 3. Characteristic diagram for inviscid supersonic contour.

the design Mach number location. The first and second derivatives of Mach number are assumed to be zero at the design Mach number and equal to the radial-flow values at the upstream end of this segment of the axis. The method of characteristics is then used to obtain the streamline defining the inviscid contour of the nozzle.

The viscous contour of the throat liner is obtained by adding the displacement thickness of the boundary layer to the inviscid contour. The boundary layer is calculated by a momentum integral method essentially like that described in [1]. The compressible friction coefficient is related to incompressible values by the van Driest II method [8] except a parabolic distribution of temperature with velocity is used. Boundary-layer parameters are obtained by integrating numerically the various equations, including those which take into account the transverse curvature effects on the boundary layer. In the power-law equation for velocity distribution, the exponent is determined as a function of Reynolds number. Finally, the solution of the momentum integral is iterated because the term involving the local nozzle radius pertains to the viscous radius which is, in turn, the result of the calculations.

Now, the skin-friction coefficient, the radius of contour, and the Reynolds number, Re , at various locations along the liner are known. Since the radius of contour at any point is known, the area can be determined. If the

area is known, the Mach number can be found from the one-dimensional isentropic tube flow equation [9]

$$\frac{A}{A^*} = \frac{1}{M} \left(\frac{1 + \frac{\gamma-1}{2} M^2}{\frac{\gamma+1}{2}} \right)^{\frac{\gamma+1}{2(\gamma-1)}} \quad (7)$$

Since this equation is implicit in Mach number, the Newton-Raphson method [10] was used to iterate and solve for the Mach number.

The velocity, u , in Eq. (5) was found from the Mach number definition [9]

$$M = \frac{u}{u_s} ,$$

where, by rearranging,

$$u = M u_s \quad (8)$$

The speed of sound, u_s , is known from the physical properties of the air, and the equation from [9] is

$$u_s = (\gamma R T)^{1/2} , \quad (9)$$

where the static temperature of the air can be calculated from the one-dimensional isentropic tube flow equation [9],

$$\frac{T}{T_0} = \left[1 + \left(\frac{\gamma-1}{2} \right) M^2 \right]^{-1} ; \quad (10)$$

therefore, the quantities in Eq. (1) are known, except the liner airside metal temperature, T_a .

Then the heat is transferred through the metal liner by means of radial conduction. This can be calculated by Fourier's law of heat conduction for a thick-walled cylinder treated as a plane wall [11]. This form of the equation allows the use of the incremental length, ΔL , in the numerator, and greatly simplifies the problem, as will be seen later. For liners which are usually very thin, this equation has an error of less than 2.2 per cent.

The equation is

$$q_K = \frac{\pi (d_2 + d_1) LK (T_a - T_w)}{d_2 - d_1} \quad (11)$$

The equation may be applied to an incremental length, ΔL , along which the axial gradient is assumed to be negligible. Also, the liner inside diameter, d_1 , and outside diameter, d_2 , can be modified to a mean radius and thickness as follows:

$$\frac{d_2 + d_1}{2} = d_m = 2 r_m ,$$

$$d_2 + d_1 = 4 r_m , \quad (12)$$

and

$$d_2 - d_1 = 2 t . \quad (13)$$

A simplified equation for radial heat transfer was obtained by substitution of incremental length and Eqs. (12) and (13) into Eq. (11). The result is

$$q_K = \frac{2 \pi r_m \Delta L K (T_a - T_w)}{t} . \quad (14)$$

The liner metal conductivity, K , usually varies with temperature. Since there is a temperature gradient through the liner thickness, the conductivity is evaluated at the average of the liner surface temperatures. This conductivity can usually be approximated by a linear equation of temperature over a limited temperature range. The constants for the linear equation are inputs to the program so that a variety of materials can be examined. These constants are determined by plotting the material conductivity in Btu-in./hr/ft²/°R on the ordinate as a function of temperature in °R along the abscissa. The slope of a line that is a linear approximation of that curve, for the desired temperature range; and, the value of the conductivity at zero temperature, establish the necessary input constants for the subroutine. Thus, all the quantities in Eq. (14) are known, except the liner surface temperatures, T_a and T_w .

The heat is then transferred radially to the cooling water by means of forced convection. Newton's law of cooling states,

$$q_w = h_w A_w (T_w - T_b) . \quad (15)$$

The area, A_w , is the outside liner circumference, c_w , times an incremental length, ΔL . The bulk temperature of the water, T_b , was assumed constant for this analysis. The bulk water temperature is an input to the program so that variations can be considered.

Considerable work has been done in the field of heat exchangers for pipes and plates. Experimental data have produced many empirical equations for heat-transfer coefficients in parallel and counterflow cooling of pipes. The parallel flow method was used to cool liners so that lower metal temperatures are obtained at the throat. Thus, the waterside heat-transfer coefficient, h_w , was approximated by [6]

$$\frac{h_w D}{k} = 0.027(Re)^{0.8} (Pr)^{1/3} \left(\frac{\mu}{\mu_w}\right)^{0.14} \quad (16)$$

The water properties are evaluated at the bulk temperature, except water viscosity at the liner surface, μ_w , which is determined at the waterside liner temperature, T_w . Reynolds number and Prandtl number are defined [6] as

$$Re = \frac{GD}{\mu}$$

and

$$Pr = \frac{C_p \mu}{k}$$

where

$$G = \rho u .$$

Substitution of these definitions into Eq. (16) and simplification of the results yield

$$h_w = 0.027 \frac{(GD)^{0.8}}{D} \left(\frac{C_p k^2}{\mu} \right)^{1/3} \left(\frac{1}{\mu_w} \right)^{0.14} . \quad (17)$$

The hydraulic diameter, D, is defined [6] as

$$D = \frac{4A}{P} , \quad (18)$$

where A is the cross-sectional area of the waterflow passage, and P is the wetted perimeter of both surfaces.

The flow area is described by

$$A = \pi (r_3^2 - r_2^2) , \quad (19)$$

and the perimeter by

$$P = 2\pi (r_3 + r_2) . \quad (20)$$

A simplified expression for D was obtained by substitution of Eqs. (19) and (20) into Eq. (18). The result is

$$D = 2 t_w , \quad (21)$$

where t_w is the thickness of the water passage.

The water properties--viscosity, density, conductivity, and specific heat--vary with temperature. These

properties are available in tables or graphs from various sources; however, they needed to be in equation form for the computer solution. Therefore, convenient property combinations were plotted for appropriate temperature ranges and polynomial equations were derived by the method of least squares. The resulting equations are:

$$\rho_c = \{ [5.38(10)^{-8} T_b - 9.89(10)^{-5}] T_b + 5.84(10)^{-2} \} T_b - 2.88, \quad (22)$$

$$\left(\frac{C_p k^2}{\mu} \right)^{1/3} = T_b [5.04(10)^{-3} - T_b(2.79)(10)^{-6}] - 1.52, \quad (23)$$

and

$$(\mu_w)^{-0.14} = T_w [3.35(10)^{-3} - T_w(1.83)(10)^{-6}] - 0.37. \quad (24)$$

The term, ρ_c is the density divided by 7.48 gal./ft³ to enable the direct substitution of the water flow rate, in gpm, into the program. The resulting units are lb_m/gallon. The units of

$$\left(\frac{C_p k^2}{\mu} \right)^{1/3}$$

are Btu/lb_m^{2/3}/hr^{1/3}/ft^{1/3}/°F. Both ρ_c and

$$\left(\frac{C_p k^2}{\mu} \right)^{1/3}$$

are evaluated at the bulk water temperature, T_b . The term $(\mu_w)^{-0.14}$ is the reciprocal of the water viscosity, μ_w , evaluated at the waterside wall temperature of the liner,

and raised to the 0.14 power. The units are $\text{ft}^{0.14} \cdot \text{hr}^{0.14} \cdot \text{lb}_m^{-0.14}$. Substitution of these equations into Eq. (17) for a known water channel thickness and water flow rate revealed that the waterside heat-transfer coefficient is only a function of the waterside metal temperature of the liner. Therefore, Eq. (15) shows that the waterside heat rate is only dependent on the waterside metal temperature. A complete radial heat flow is defined using Eqs. (1), (14), and (15). For negligible radiation and axial conduction, the equality

$$q_a = q_K = q_w \quad (25)$$

must hold. Thus, using the definitions of these heat rates, one can show that

$$h_a A_a (T_r - T_a) = \frac{2\pi r_m \Delta L K (T_a - T_w)}{t} = h_w A_w (T_w - T_b) .$$

The above identity was simplified by using the area equations developed previously. The result obtained was

$$h_a r_1 (T_r - T_a) = \frac{r_m K (T_a - T_w)}{t} = h_w r_2 (T_w - T_b) . \quad (26)$$

This is the general identity that the radial heat-transfer solution must satisfy for the entire length of the nozzle. From this identity the equations that have been programmed were developed.

For computation purposes, the previous identity was divided into two equations. The first, an equation for T_a , was derived by setting the airside heat-transfer rate, q_a , equal to the conductivity heat-transfer rate, q_K . The result was

$$h_a r_1 (T_r - T_a) = \frac{r_m K (T_a - T_w)}{t},$$

or, rearranging,

$$T_a = \frac{h_a r_1 T_r + \frac{r_m K T_w}{t}}{\frac{r_m K}{t} + h_a r_1}. \quad (27)$$

The second equation, an expression for T_w , was obtained by setting the conductivity heat transfer equal to the water-side heat transfer. The result was

$$h_w r_2 (T_w - T_b) = \frac{r_m K (T_a - T_w)}{t},$$

or, rearranging,

$$T_w = \frac{\frac{r_m K T_a}{t} + h_w r_2 T_b}{h_w r_2 + \frac{r_m K}{t}}. \quad (28)$$

The necessary equations now exist to determine the surface temperatures of the metal liner at any point. A step-by-step procedure of how the equations are used is as follows:

1. An initial airside metal temperature and water-side heat-transfer coefficient is assumed.
2. The waterside metal temperature is calculated from Eq. (28).
3. A viscosity of water is calculated from Eq. (24).
4. A waterside heat-transfer coefficient is calculated from Eq. (17).
5. A metal conductivity is calculated substituting an average of the assumed airside metal temperature and the calculated waterside metal temperature into the linear conductivity equation.
6. A new airside metal temperature is calculated from Eq. (27).
7. Compare airside metal temperature in step (1) to that in step (6).
 - A. If they differ by more than an acceptable deviation, return to step (1) and use the value calculated in step (6) and iterate.
 - B. If their deviation is acceptable, stop iteration.

CHAPTER III SUBSONIC HEAT-TRANSFER ANALYSIS

Bartz [4, 5] concluded that the boundary-layer thickness in the subsonic section of a nozzle had very little effect on the supersonic side boundary-layer or heat-transfer coefficient; also, that the heat-transfer coefficient on the subsonic side was only slightly affected by the boundary-layer thickness. Based on these conclusions, empirical equations were used to solve for the subsonic heat-transfer coefficient.

A smooth, continuous inside surface contour for the subsonic section of the liner was a design criterion for more uniform heat transfer and flow. This is substantiated by Back, Massier, and Cuffel [12], and discussed by Sivells [3]. To try to meet this requirement a set of polynomial equations were derived to describe the various regions leading up to the liner throat. General equations that can be used for many different throat liners are derived in Appendix A.

Subsonic one-dimensional tube flow relationships are usually developed using the throat conditions as a reference. Since this program calculates the supersonic liner conditions first, which includes the throat, it would be advantageous to also use the throat conditions as reference for developing the subsonic heat-transfer

analysis. The same heat-balance methods used in Chapter II will be used here, except the liner airside heat-transfer coefficient, h_a , will be approximated by empirical equations. Bartz [4, 5] suggests a simple equation

$$h_a = \left[\frac{0.026}{D^{0.2}} \left(\frac{\mu^{0.2} C_p}{Pr^{0.6}} \right) \left(\frac{Pc \cdot g}{C^*} \right) \left(\frac{D}{R^*} \right)^{0.1} \right] \left(\frac{A^*}{A} \right)^{0.9} \sigma, \quad (29)$$

where

$$\sigma = \frac{1}{\left[\frac{1}{2} \frac{T_a}{T_o} \left(1 + \frac{\gamma-1}{2} M^2 \right) + \frac{1}{2} \right]^{0.6} \left(1 + \frac{\gamma-1}{2} M^2 \right)^{0.15}}. \quad (30)$$

Bartz also indicates that the term in brackets in Eq. (30) remains relatively constant through the nozzle. This suggests the ratio of airside heat-transfer coefficient at any point divided by the airside heat-transfer coefficient at the throat, h_a^* . The results of that ratio, using Eq. (30), is

$$\frac{h_a}{h_a^*} = \left(\frac{A^*}{A} \right)^{0.9} \left(\frac{\sigma}{\sigma^*} \right). \quad (31)$$

At the throat the Mach number, M , is one. Thus,

$$\sigma^* = \frac{1}{\left[\frac{1}{2} \frac{T_a^*}{T_o} \left(1 + \frac{\gamma-1}{2} \right) + \frac{1}{2} \right]^{0.6} \left(1 + \frac{\gamma-1}{2} \right)^{0.15}}. \quad (32)$$

Since T_a^* will be determined by the supersonic analysis, σ^*

will also be known. Therefore, an iteration involving T_a will be required to determine σ . Equation (30) also shows that σ is a function of the local Mach number, M ; however, the one-dimensional tube flow equation may be used to determine the local Mach number from the known area ratio that is developed in Appendix A. Equation (7) of Chapter II is the required equation, and again, the Newton-Raphson method can be used to solve for Mach number.

Thus, the radial temperature distribution through the liner thickness can be evaluated using Eqs. (7), (31), and (32), and the procedure described in Chapter II.

CHAPTER IV
STRESS ANALYSIS
Thermal Stresses

Thermal stresses were calculated using the long, hollow-cylinder equations assuming a radial logarithmic temperature distribution [13]. Generally, the total stresses will be desired which should be a maximum at the inside, or outside, radius. Thus, at r_1 , the circumferential and axial stresses are described by

$$\sigma_{\theta} = \sigma_z = \frac{\alpha E \Delta T \left[1 - \frac{2r_2^2 \ln \left(\frac{r_2}{r_1} \right)}{r_2^2 - r_1^2} \right]}{2(1-\mu) \ln \left(\frac{r_2}{r_1} \right)}, \quad (33)$$

and the radial stress by

$$\sigma_r = 0. \quad (34)$$

At r_2 , the circumferential and axial stresses are

$$\sigma_{\theta} = \sigma_z = - \frac{\alpha E \Delta T \left[1 - \frac{2r_1^2 \ln \left(\frac{r_2}{r_1} \right)}{r_2^2 - r_1^2} \right]}{2(1-\mu) \ln \left(\frac{r_2}{r_1} \right)}, \quad (35)$$

and the radial stress is

$$\sigma_r = 0 . \quad (36)$$

The coefficient of expansion, α , modulus of elasticity, E , and Poisson ratio, μ , are generally constant for the metal temperatures encountered and no functional equations of temperature are required; but, they are inputs to the program. These values are evaluated at the airside temperature, T_a , of the liner for conservatism. These equations account for a radial temperature distribution only.

Subsonic Pressure Stresses

The stresses due to internal pressure are calculated by thick-walled pressure vessel theory [13]. At the inside surface, r_1 , the circumferential stress equation is

$$\sigma_\theta = \frac{P_\infty (r_2^2 + r_1^2)}{r_2^2 - r_1^2} , \quad (37)$$

and the radial stress equation is

$$\sigma_r = -P_\infty . \quad (38)$$

At r_2 , the circumferential stress equation is

$$\sigma_\theta = \frac{2 P_\infty r_1^2}{r_2^2 - r_1^2} , \quad (39)$$

and the radial stress equation is

$$\sigma_r = 0 . \quad (40)$$

The axial stress due to internal pressure is uniform across the thickness, and the equation is

$$\sigma_z = \frac{F_a}{\pi (r_2^2 - r_1^2)} , \quad (41)$$

where r_2 and r_1 are arbitrary outside and inside liner radii, respectively, depending on the desired location. The average axial force, F_a , equation is developed in Appendix B.

The stresses in the liner due to water pressure were calculated by thick-walled pressure vessel equations from [13]. At the inside surface of the liner, r_1 , the circumferential stress equation is

$$\sigma_\theta = - \frac{2 P_w r_2^2}{r_2^2 - r_1^2} , \quad (42)$$

and the radial stress equation is

$$\sigma_r = 0 . \quad (43)$$

At the outside surface, r_2 , the circumferential stress equation is

$$\sigma_{\theta} = - \frac{P_w (r_2^2 + r_1^2)}{r_2^2 - r_1^2} , \quad (44)$$

and the radial stress equation is

$$\sigma_r = -P_w . \quad (45)$$

The axial stress is uniform across the liner thickness, and the equation is

$$\sigma_z = \frac{F_w}{\pi (r_2^2 - r_1^2)} . \quad (46)$$

The axial load, F_w , equation is derived in Appendix B.

Supersonic Pressure Stresses

The equations for stresses due to air and water pressure in the supersonic side of the liner are the same as the equations for the subsonic stress. However, the axial loads, F_a and F_w , are different and are derived in Appendix B.

Total Stresses

The method of superposition is used to total all stresses where appropriate, and these totals are then substituted into a theory of failure equation, known as the distortion-energy theory [14]. This is the best theory to use for ductile materials, and it predicts the beginning of

yielding for a triaxial stress state. The total stress equation is

$$\sigma_y = \left\{ \frac{1}{2} [(\sigma_\theta - \sigma_r)^2 + (\sigma_\theta - \sigma_z)^2 + (\sigma_z - \sigma_r)^2] \right\}^{\frac{1}{2}} . \quad (47)$$

The maximum calculated value of σ_y for the entire liner should be used to check the structural integrity of the proposed design. If the liner material yield strength at airside temperature is less than or equal to the above calculated yield strength, the liner will probably permanently deform. To design for this, a safety factor is multiplied times the above calculated yield strength and the yield strength of the candidate material at airside temperature, T_a , must exceed that product.

Based on these criteria, experience has shown that these stress design criteria are adequate for liner design.

CHAPTER V SUMMARY AND RECOMMENDATIONS

The result of this study is a subroutine, HEAT, that can be added to a boundary-layer program and analyze the aerodynamic and primary structural capabilities of candidate liners. The HEAT subroutine uses basic heat transfer and stress theory, making the results easily understood.

Because of the many iterations required to solve this problem, previous analysis by hand calculations took weeks to complete. Using the HEAT subroutine, one should be able to reduce the solution time to days, which would allow a more complete optimization of candidate materials. Also, the probability of errors should be decreased because of the computer.

There are primarily two requirements that should be met in liner design using this computerized method. They are:

1. The yield strength of the candidate liner should be greater at airside metal temperature than the product of the maximum calculated yield stress and a safety factor.
2. The water pressure of the available cooling water supply at the point in question should be greater than the product of the saturated water

pressure found in a standard steam table at the waterside wall temperature and the desired safety factor.

This second requirement keeps local hot spots from developing by preventing water cavitation.

Of course, there are other factors to consider, such as cooling-water pressure loss through the entire circuit, volume of cooling water required, cost of liner material, and minimum thickness of the liner to facilitate machining and handling.

Although this program was written for a specific type of problem, a liner with one end fixed and the other end free, the capability of determining the axial temperature gradient by selecting a small increment of points to be analyzed could be very useful for the study of liners with various end conditions. Not only can liner design be optimized, but cooling water conditions might also be improved.

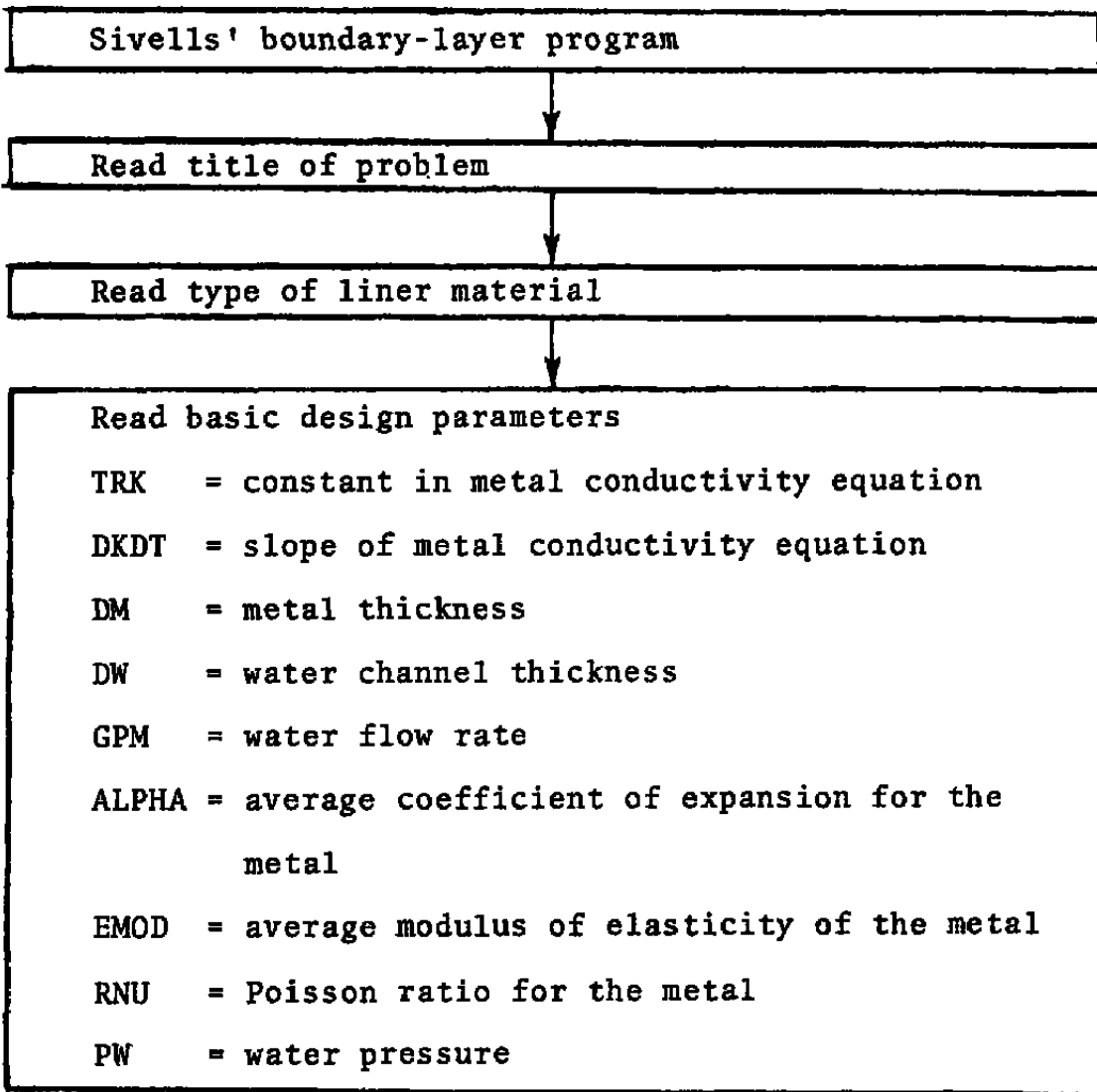
The boundary-layer properties calculated in this design analysis program are based on turbulent theory. However, many references indicate that there exist two boundary layers; a very thin laminar layer with the turbulent layer on top of it. Possible improvements could be made in heat-transfer analysis if the boundary layer is

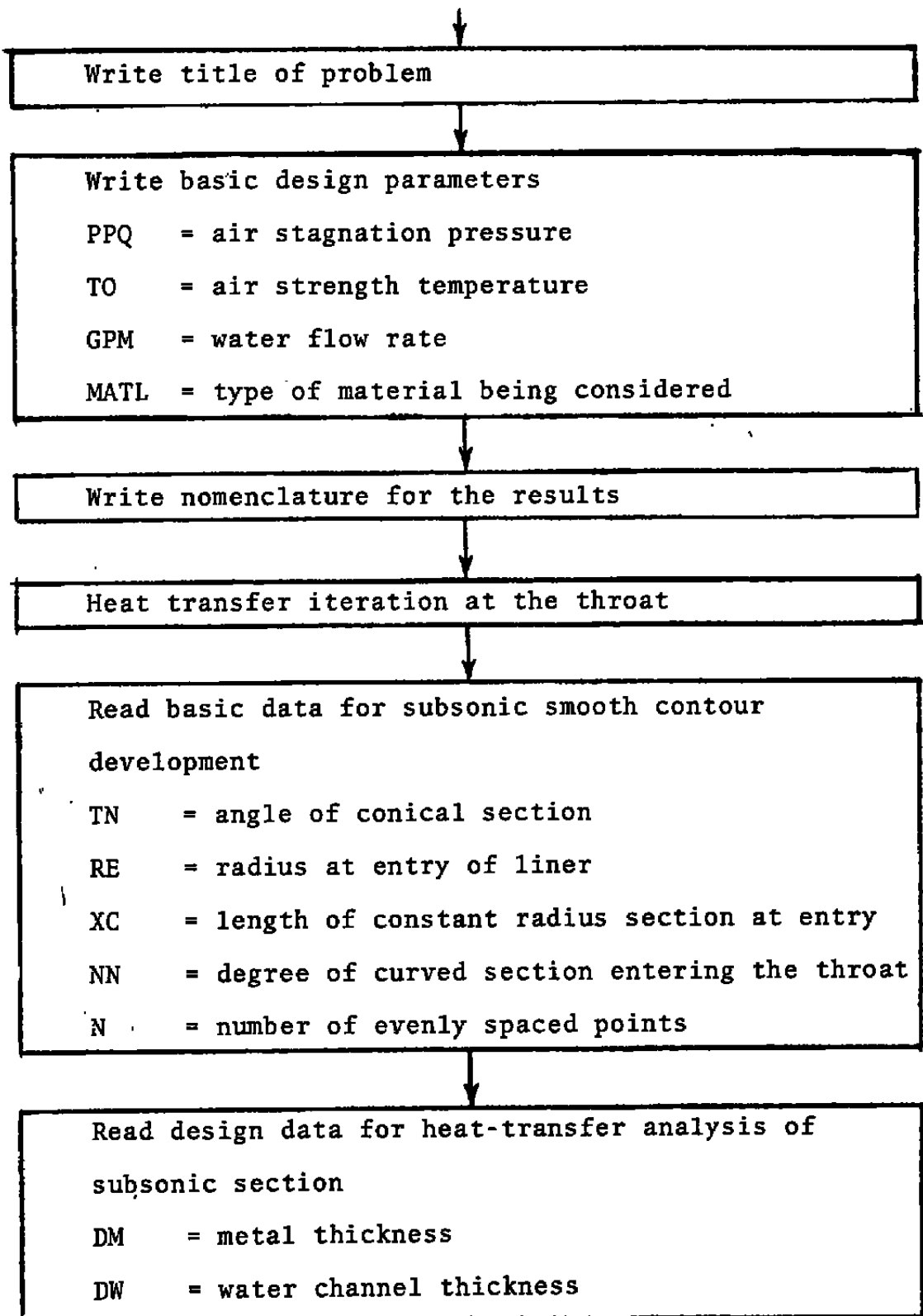
accounted for. Once the double boundary-layer solution is programmed, however, the HEAT subroutine could still be used to perform the heat-transfer and stress analysis.

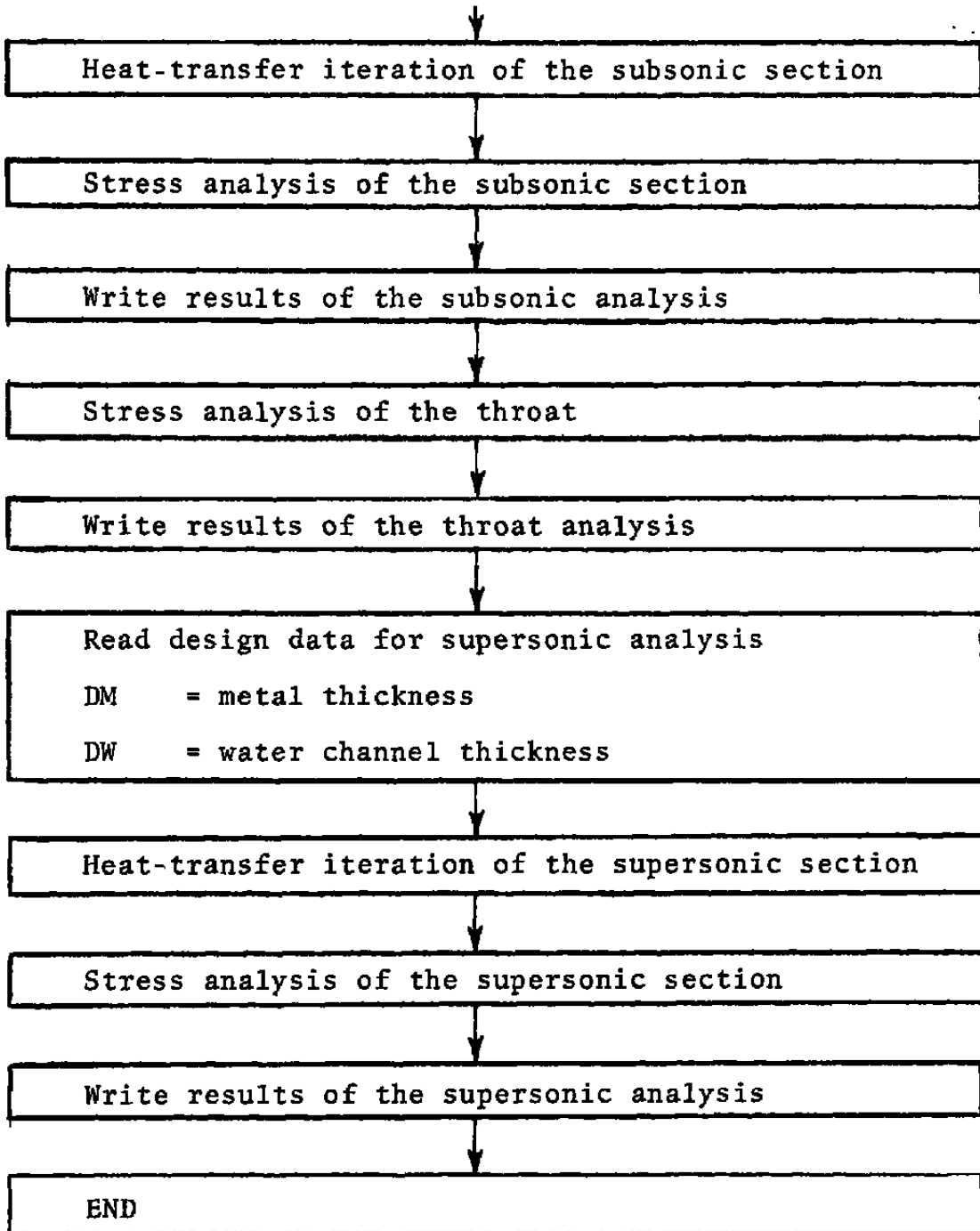
CHAPTER VI HEAT SUBROUTINE

A basic outline of the subroutine HEAT is presented in this chapter in block diagram form; then a complete listing of the subroutine is given.

Block Diagram








```

R2=R1+ DM
R3=R2+ DW
PPG=(5.382269D-8+TB-9.8865595D-5)*TB+5.8421053D-2)*TB-2.876661D+0
GDR=1.44D+3*GPM*PPG/PI
GD=GDR/(R3+R2)
HD=(R3-R2)/6.0+0
CPKMU=TB*(5.03977D-3-TB*2.78826D-6)-1.51868D+0
HWMU=2.3D-2*CPKMU*GD**8.D-1/HD/3.6D+3
TRM=1.44D+4*(R2-R1)/(R2+R1)
1 IPJ=IPJ+1
TWQ=(HAIR*TAW+QFUN*(TWT-15.0+0))/(HAIR+QFUN)
FAIR=TRM*HAIR*R1*(TAW-TWQ)
TWQK=TWQ*DKDT+TRK
TWW=(TWQ*(TWQK+TRK)-FAIR)/(DSQRT(TWQK**2-DKDT*FAIR)+TRK)
FCOND=(DKDT*TWW+TWQK+TRK)/TRM
RMU14=TWW*(3.3474D-3-TWW*.82823D-6)-.368957D+0
HWAT=HWMU*RMU14
QFUNW=ONE/(ONE/HWAT/R2+ONE/FCOND)/H1
IF (IV.GT.1.AND.IV.LT.IW) RETURN
IF (DABS(TWT-TWQ).LT.1.D-2.AND.DABS(QFUN-QFUNW).LT.1.D-5) GO TO 2
RETURN
2 IF (IV.LT.IW) RETURN
C
C THE NEXT SECTION CALCULATES THE SUBSONIC CONTOUR AND THEN THE
C COMPLETE ANALYSIS OF THE SUBSONIC SECTION
SIGT=1./((((1./G9+1.)*(TWT/(2.*TO)))**.5)**.6)*((1./G9+1.)**.15))
HAIRT=HAIR
RG=69+.1D+0
READ (5,1) TN,RE,XC,NN,N
RS=RC(1)
XL=S(1)
IF (TN.GT.4.D+0) TN=DTAN(TN*PI/1.8D+2)
RI=RE
XLC=XL-XC
RIS=RE-RS
NM1=NN-1
NM2=NN-2
NP=.5D+0*NN*NM1
RB=NM1*RC*TN**2/NN/NM2**2
FRN=NM1*RS*RC/NM2
Z1=FRN*TN
XLCM=2.D+0*RIS/TN-Z1/NN
IF (XLCM.LT.XLC) TN=.1D+0*RIS/(DSQRT(8.D+0*RIS*FRN/NN*XLC**2)+XLC)
Z1=FRN*TN
X1=2.D+0*(XLC-RIS/TN)-NM1*Z1/NN
HX1=.5D+0*X1
AA=HX1*TN
R=RE
DX=XL/N
DO 8 JJ=1,N
X=UX*(JJ-1)
IF (X.LE.XC) GO TO 5
IF (X.GT.X1+XC) GO TO 3
XR=(X-XC)/X1
C
C ENTRANCE FOURTH ORDER CONTOUR EQUATION

```

```

R=RE-AA*(2.0+0-XR)*XH**3
GO TO 5
3. IF (X.GT.XL-Z1) GO TO 4
C
C CONICAL CONTOUR EQUATION
R=RE+AA-TN*(X-XC)
GO TO 5
4 ZR=(XL-X)/Z1
ZRN=ZR**NM2
C
C THIRD OR FOURTH ORDER EQUATION LEADING TO THROAT
C
R=HS*(1.0+0+BB*(NP-ZRN)*ZR**2 )
5 AB=RG5*((R/RS)**2)**RGA
CM=G9/AB
C
C SUBSONIC MACH NUMBER ITERATION
6 FQ=(G9+CM**RG5-CM*AB)/(RG5*CM**G9-AB)
CM=CM-FQ
IF (DABS(FQ).GT.1.0-9) GO TO 6
XM=CM**GA
IF (X.EQ.0.0) XM1 = XM
PEN=PPQ*(1.+(GM/2.0)*(XM1**2))**(-GAM/GM)
READ (5,18) DMB,DWB
R2B = R + DMB
R3B = R2B + DWB
TS=TO/(1.0 + (GM/2.0)* XM**2.0)
TRC = .87*(TO-TS)+TS
RMB = (R2B +R)/2.0
TRMB= DMB/RMB
GD = GDR/ (R3B+R2B)
HWMU=7.30-2*CPKMU*GD**8.0-1/HD/3.60*3
HWB = HWMU * RMU14
CD = TRK + DKDT * TWT
TAB = TWT
7 TABA = TAB
SIGI=(((XM**2/G9+1.)*(TABA/(2.*TO))+.5)**.6)*((XM**2/G9+1.1
1**15)
SIG=1./SIGI
HAB= ((RCO(1)/R)**1.8)* HART *(SIG/SIGI)
HART = 3600.*(HAB*R+R2B*TRMB/CD)+R2B
TWB = (TB*HWB*HART+HAB*R*TRC)/(HAB*R + HWB * HART)
RMU14 =TWB *(3.34740-3-TWB *1.828230-6)-.3689570*0
HWB = HWMU * RMU14
TBAR = (TWB +TABA)/2.0
CD = TRK + DKDT * TBAR
TAB = 3600.*(HWB*R2B*DMB*(TWB -TB))/(CD*RMB) + TWB
IF (DABS( TABA- TAB).GT.1.0-2) GO TO 7
PAB=(.5*PPQ*((1.0+(GM/2.0)*(XM1**2))**(-GAM/GM))+(1.0+(GM/2.0)*
1*(XM**2)**(-GAM/GM)))
PA = PAB
FA= PI*((R**2-RE**2)*PA+PEN*(RE**2-R4**2))
FW= PI*PW*(R5**2-R2B**2)
R0 = R2B
R1 = R
TGRAD = TAB - TWB

```

```

C      THERMAL STRESS EQUATIONS
C
  STHI = (TGRAD*ALPHA*EMOD*(1.0-(2.0*RO**2*DLOG(RO/RI)/(RO**2-RI**2
1))))/(2.0*(1.0-RNU)*DLOG(RO/RI))
  STHO = (TGRAD*ALPHA*EMOD*(1.0-(2.0*RI**2*DLOG(RO/RI)/(RO**2-RI**2
1))))/(2.0*(1.0-RNU)*DLOG(RO/RI))
  STAO = STHO
  STAI = STHI
C
C      PRESSURE STRESS EQUATIONS
C
  SAHI = (PA*(RI**2+RO**2))/(RO**2-RI**2)
  SAHO = (2.0* RI**2*PA)/(RO**2-RI**2)
  SAA = FA / (PI * ( RO**2 - RI**2))
  SWA = FW / (PI * ( RO**2 - RI**2))
  SWHI = (2.0 * RO**2 * PW)/(RI**2 - RO**2)
  SWHO = (PW * (RO**2 + RI**2))/(RI**2 - RO**2)
C
C      THEORY OF FAILURE STRESS EQUATIONS
C
  STYO = (.5*((STHO + SAHO + SWHO + PW)**2 + (STHO + SAHO + SWHO -
1  STAO - SAA - SWA)**2 + (-PW - STAO - SAA - SWA)**2)**.5
  STYI = (.5*((STHI + SAHI + SWHI + PA)**2 + (STHI + SAHI + SWHI -
1  STAI - SAA - SWA)**2 + (-PA - STAI - SAA - SWA)**2)**.5
  WRITE (8, 9)  X,R,R2B,R3B,HAR,HWB,CD,TAB,TWB,TRC,STHI,STHO,STAI,
1              STAO,SAHI,SAHO,SAA,SWHI,SWHO,SWA,STYI,STYO
C
C      CONTINUE
C
C      NEXT THE STRESS ANALYSIS IS MADE FOR THE THROAT
C
  CU=FCOND*TRM/2.D*0
  TGRAD = TWI - TWB
  R2=RCO(IJ)* DM
  R3=R2* DW
  RO = R2
  RI = RCO(IJ)
  PA = (PPQ*(SPR(IJ)+ SPR(1))*.5)
  FA = -(.5*PPQ*(1.+SPR(1))*PI*(RE**2-(RCO(1))**2))-PI*PEN*(R4**2
1-RE**2)+PI*PA*((RCO(IJ))**2-(RCO(1))**2)
  FW = PI*PW*(R5**2-R2 **2)
C
C      THERMAL STRESS EQUATIONS
C
  STHI = (TGRAD*ALPHA*EMOD*(1.0-(2.0*RO**2*DLOG(RO/RI)/(RO**2-RI**2
1))))/(2.0*(1.0-RNU)*DLOG(RO/RI))
  STHO = (TGRAD*ALPHA*EMOD*(1.0-(2.0*RI**2*DLOG(RO/RI)/(RO**2-RI**2
1))))/(2.0*(1.0-RNU)*DLOG(RO/RI))
  STAO = STHO
  STAI = STHI
C
C      PRESSURE STRESS EQUATIONS
C
  SAHI = (PA*(RI**2+RO**2))/(RO**2-RI**2)
  SAHO = (2.0* RI**2*PA)/(RO**2-RI**2)
  SAA = FA / (PI * ( RO**2 - RI**2))
  SWA = FW / (PI * ( RO**2 - RI**2))

```

```

SWHI = (2.0 * RO**2 * PW)/(RI**2 - RO**2)
SWHO = (PW * (RO**2 + RI**2))/(RI**2 - RO**2)
C
C
THEORY OF FAILURE STRESS EQUATIONS
C
1 STYO = (.5*((STHO + SAHO + SWHO + PW)**2 + (STHO + SAHO + SWHO -
   STAO - SAA - SWA)**2 + (-PW - STAO - SAA - SWA)**2))**.5
1 STYI = (.5*((STHI + SAHI + SWHI + PAI)**2 + (STHI + SAHI + SWHI -
   STAI - SAA - SWA)**2 + (-PA - STAI - SAA - SWA)**2))**.5
1 WRITE (8,19) SL(IJ),RCO(IJ),R2,R3,HAIR,HWAT,CD,TWT,TWW,TAW,STHI,
1 STHO,STAI,STAO,SAHI,SAHO,SAA,SWHI,SWHO,SWA,STYI,STYO
RETURN
9 CONTINUE
C
C
NOW THE HEAT TRANSFER AND STRESS ANALYSIS IS MADE ON THE
C SUPERSONIC SECTION OF THE LINER
C
READ (5,18) DM,DW
PI=2.0*0.0DARSIN(ONE)
R2=RCO(IJ)*DM
R3=R2*DW
TRM=1.44D+4*DM/(R2+RCO(IJ))
HD=DW/6.D+0
GD=GDR/(R3+R2)
HWMU=2.3D-2*CPKMU*GD**8.D-1/HD/3.6D+3
HWAT=HWMU*RMU14
TBAR = (TWT + TWW)/2.
CD = TRK + DKDT * TBAR
10 TA=TWT
TWW=TA
TWW=(2.*CD*TWG/TRM+HWAT*R2*TB)/(2.*CD/TRM+HWAT*R2)
RMU14=TWW*(3.3474D-3-TWW*1.82823D-5)-.368957D+0
HWAT=HWMU*RMU14
TBAR = (TWG + TWW)/2.
CD = TRK + DKDT * TBAR
TA=(2.*CD*TWW/TRM+HAIR*RCO(IJ)*TAW)/(2.*CD/TRM+HAIR*RCO(IJ))
IF (DABS(TWQ-TA).GT.1.D-2) GO TO 10
TGHAD = TA - TWW
RO = R2
RI = RCO(IJ)
PA = (PPQ*(SPR(IJ) + SPR(1))*.5)
FA = -(.5*PPQ*(1.+SPR(1))*PI*(RE**2-(RCO(1))**2))-PI*PEN*(R4**2
1-RE**2)*PI*PA*((RCO(IJ))**2-(RCO(1))**2)
FW= PI*PW*(R5**2-R2 **2)
C
C
THERMAL STRESS EQUATIONS
C
1 STHI = (TGRAD*ALPHA*EMOD*(1.0-(2.0*RO**2*DLOG(RO/RI)/(RO**2-RI**2
1))))/(2.0*(1.0-RNU)*DLOG(RO/RI))
1 STHO = (TGRAD*ALPHA*EMOD*(1.0-(2.0*RI**2*DLOG(RO/RI)/(RO**2-RI**2
1))))/(2.0*(1.0-RNU)*DLOG(RO/RI))
STAO = STHO
STAI = STHI
C
C
PRESSURE STRESS EQUATIONS
C

```

```

SAHI = (PA*(RI**2+RO**2))/(RO**2-RI**2)
SAHO = (2.0* RI**2*PA)/(RO**2-RI**2)
SAA = FA / (PI * ( RO**2 - RI**2))
SWA = FW / (PI * ( RO**2 - RI**2))
SWHI = (2.0 * RO**2 * PW)/(RI**2 - RO**2)
SWHO = (PW * (RO**2 + RI**2))/(RI**2 - RO**2)

```

C
C
C

THEORY OF FAILURE STRESS EQUATIONS

```

STYO = (.5*((STHO + SAHO + SWHO + PW)**2 + (STHO + SAHO + SWHO -
1 STAO - SAA - SWA)**2 + (-PW - STAO - SAA - SWA)**2))**.5
STYI = (.5*((STHI + SAHI + SWHI + PA)**2 + (STHI + SAHI + SWHI -
1 STAI - SAA - SWA)**2 + (-PA - STAI - SAA - SWA)**2))**.5
WRITE (8,19) SL(IJ),RCD(IJ),R2,R3,HAIR,MWAT,CD,TA,TW,TAW,STHI,
1 STHO,STAI,STAO,SAHI,SAHO,SAA,SWHI,SWHO,SWA,STYI,STYO
RETURN
11 FORMAT (20A4)
12 FORMAT (11E7,0)
13 FORMAT (1H1,////////15X,' COMPUTER OUTPUT - EXAMPLE PROBLEM',////
115X,' HEAT TRANSFER AND STRESS ANALYSIS SUMMARY',/16X,20A4////)
14 FORMAT (1H0,////////15X,' ***DESIGN CONDITIONS***',//15X,' STAGNA
1TION PRESSURE (PSI) =',F10,2,//15X,' STAGNATION TEMPERATURE (D
2EG.R)=' ,F10,2,//15X,' COOLING WATER FLOW RATE (GPM) =',F10,2,//15X
3,' COOLING WATER PRESSURE (PSI) =',F10,2,//15X,' LINER MATERIAL-'
4,20A4)
15 FORMAT (1H1,//// 15X,' ***NOMENCLATURE FOR RESULTS***',//15X,'
1 X - LOCATION OF POINT BEING ANALYZED (IN.)',//15X,' R1 - INSIDE
2LINER RADIUS (IN.)',//15X,' R2 - OUTSIDE LINER RADIUS (IN.)',//15X
3,' R3 - INSIDE RADIUS OF COOLING WATER HOUSING (IN.)',//15X,' HA -
4 LINER AIRSIDE HEAT TRANSFER COEFFICIENT (BTU/SEC/SQ.FT./DEG.F)',/
5/15X,' HW - LINER WATERSIDE HEAT TRANSFER COEFFICIENT (BTU/SEC/SQ.
6FT./DEG.F)',//15X,' CD - LINER METAL CONDUCTIVITY (BTU-IN./HR/SQ.F
7T./DEG.F)',//15X,' TA - LINER AIRSIDE METAL TEMPERATURE (R)')
16 FORMAT (1H0,14X,' TW - LINER WATERSIDE METAL TEMPERATURE (R)',//15
1X,' TR - LINER AIRSIDE BOUNDARY LAYER RECOVERY TEMPERATURE (R)',//
215X,' STHI - LINER AIRSIDE THERMAL CIRCUMFERENTIAL STRESS (PSI)',/
3/15X,' STHO - LINER WATERSIDE THERMAL CIRCUMFERENTIAL STRESS (PSI)
4',//15X,' STAI - LINER AIRSIDE THERMAL AXIAL STRESS (PSI)',//15X,'
5 STAO - LINER WATERSIDE THERMAL AXIAL STRESS (PSI)',//15X,' SAHI
6- LINER AIRSIDE AIR PRESSURE CIRCUMFERENTIAL STRESS (PSI)',//15X,'
7 SAHO - LINER WATERSIDE AIR PRESSURE CIRCUMFERENTIAL STRESS (PSI)'
8,//15X,' SAA - LINER AIR PRESSURE AXIAL STRESS (PSI)',//15X,' SWH
9I - LINER AIRSIDE WATER PRESSURE CIRCUMFERENTIAL STRESS (PSI)',//1
85X,' SWHO - LINER WATERSIDE WATER PRESSURE CIRCUMFERENTIAL STRESS
1(PSI)',//15X,' SWA - LINER WATER PRESSURE AXIAL STRESS (PSI)',//1
25X,' STYI - LINER AIRSIDE VON MISES-HENKY THEORY OF FAILURE YIELD
3STRESS (PSI)',//15X,' STYO - LINER WATERSIDE VON MISES-HENKY THEOR
4Y OF FAILURE YIELD STRESS (PSI)')
17 FORMAT (3E12,0,2I4)
18 FORMAT (2E8,0)
19 FORMAT (1H1,// 16X,' * * * * *',//16X,' LOCATION AND RADIUS:',/26
1X,' X(IN)=' ,F12,4,//62X,' R1(IN)=' ,F12,4,//62X,' R2(IN)=' ,F12,4,//
262X,' R3(IN)=' ,F12,4,////16X,' HEAT TRANSFER RESULTS: HA(BTU/
35EC/SQ.FT./DEG.F)=' ,F12,4,//44X,' HW(BTU/SEC/SQ.FT./DEG.F)=' ,F12,4
4,//41X,' CD(BTU-IN./HR/SQ.FT./DEG.F)=' , F12,4,//59X,' TA(DEG.R)='
5,F10,2,//59X,' TW(DEG.R)=' ,F10,2,//59X,' TR(DEG.R)=' ,F10,2,////16X

```

```
6, STRESS RESULTS: ,17X, THERMAL---STHI(PSI)= ,F8.0//59X, STHO(P  
7SI)= ,F8.0//59X, STAI(PSI)= ,F8.0//59X, STAO(PSI)= ,F8.0//49  
8X, PRESSURE---SAHI(PSI)= ,F8.0//59X, SAHU(PSI)= ,F8.0//60X, SA  
9A(PSI)= ,F8.0//59X, SWHI(PSI)= ,F8.0//59X, SWHO(PSI)= ,F8.0//  
160X, SWA(PSI)= ,F8.0//44X, VON MISES-HENCKY THEORY OF FAILURE  
2, //59X, STYI(PSI)= ,F8.0//59X, STYU(PSI)= ,F8.0//16X, * * *  
3 * * *)
```

END

CHAPTER VII
INSTRUCTIONS FOR HEAT USERS
Subroutine Function

This computer subroutine is written in Fortran IV language for use with the IBM 370/165 computer. Double precision was used so that accuracy of boundary-layer thicknesses would be maintained. Much of the nomenclature agrees with that used by Sivells [1] so that computer storage and calculation time could be minimized.

The subroutine will perform a heat-transfer and stress analysis on a wind tunnel metal liner when combined with a program that will determine the supersonic turbulent boundary-layer properties. The effects of temperature change on air, water, and liner material properties are accounted for by means of interpolated equations. The liner conductivity can be varied or remain constant by means of input constants to a linear equation. Any number of evenly spaced points can be analyzed on the liner. Any number of problems can be solved in one computer run.

Input Data

The data defining a problem for HEAT is input by computer cards. A description of each type of input data card follows. Location of data fields on the card for each

item of input is given by column numbers. The data type is indicated as INTEGER or DECIMAL, except for identification cards. INTEGER data are fixed point numbers, which must be placed as far to the right as possible in the field. DECIMAL data are floating point numbers, which may be placed anywhere in the field and must have a decimal point.

Card 1

Columns	Input	Comments
1-80	Title	Identify the problem so that the results may be labeled.

Card 2

1-80	Material	Identify the material.
------	----------	------------------------

Card 3

1-7	TRK	(DECIMAL) Material conductivity constant, Btu-in./hr/ft ² /°F.
8-14	DKDT	(DECIMAL) Slope of conductivity curve. Use zero if the conductivity remains constant with temperature.
15-21	DM	(DECIMAL) Liner throat metal thickness, inch.

Card 3

Columns	Input	Comments
22-28	DW	(DECIMAL) Water-channel thickness at the throat, inch.
29-35	R4	(DECIMAL) Liner air seal of upstream flange, inch.
36-42	R5	(DECIMAL) Liner water seal of upstream flange, inch.
43-49	GPM	(DECIMAL) Water flow rate, gpm.
50-56	ALPHA	(DECIMAL) Liner material coefficient of expansion, in./in./°F (scientific notation).
57-63	EMOD	(DECIMAL) Liner material modulus of elasticity, psi (scientific notation).
64-70	RNU	(DECIMAL) Liner material, Poisson ratio.
71-77	PW	(DECIMAL) Water pressure, psi.

Card 4

Columns	Input	Comments
1-12	TN	(DECIMAL) Angle of conical section, degree.
13-24	RE	(DECIMAL) Entry radius of subsonic section, inch.
25-36	XC	(DECIMAL) Length of constant radius of subsonic entry section, inch.
37-40	NN	(INTEGER) Order of throat entry curve equation.
41-44	N	(INTEGER) Number of evenly spaced points to be analyzed in the subsonic section.

Card 5

1-8	DM	(DECIMAL) Liner metal thickness beginning with the farthest upstream subsonic point, inch.
-----	----	---

Card 5

Columns	Input	Comments
9-16	DW	(DECIMAL) Water channel thickness beginning with farthest upstream subsonic point, inch.

All of the above cards must be input for each problem considered. Place each group of problem cards after the previous group for multiproblems.

CHAPTER VIII EXAMPLE PROBLEM

In this chapter, an example problem is solved using the HEAT subroutine with Sivells' supersonic boundary-layer program. It is solved on an IBM 370/165 computer. For input requirements to Sivells' program refer to [3]. The problem is a proposed liner to be installed in the Tunnel "C" system of the VKF at AEDC. Only one material was considered and only two points upstream and downstream of the throat were considered. The points considered are depicted on Fig. 1, page 3.

The design input data to Sivells' program was:

Card 1

Columns	Input	Example Value
2-12	Title	Mach 4

Card 2

1-10	GAM	1.4
11-20	AR	1716.575
21-30	ZO	1.0
31-40	RO	0.896
41-50	VISC	2.26968E-8
51-60	VISM	198.72

Card 3

Columns	Input	Example Value
1-10	ETAD	8.67
11-20	RC	6.0
21-30	FMACH	0.0
31-40	BMACH	3.0
41-50	CMC	4.0
51-60	SF	12.25
61-70	PP	60.0

Card 4

1-5	MT	31.0
6-10	NT	21.0
11-15	IX	0.0
16-20	IN	10.0
21-25	IQ	1.0
26-30	MD	31.0
31-35	ND	39.0
36-40	NF	61.0
41-45	MP	0.0
46-50	MQ	-1.0
51-55	JB	1.0
56-60	JX	-1.0
61-65	JC	0.0
66-70	IT	0.0
71-75	LR	21.0
76-80	NX	13.0

Card 5

Columns	Input	Example Value
1-10	PPQ	211.0
11-20	TO	1638.0
21-30	TWT	900.0
31-40	TWAT	540.0
41-50	QFUN	0.1
51-60	ALPH	0.0
61-65	IHT	20.0
66-70	IR	0.0
71-75	ID	-1.0
76-80	LV	5.0

The following were input into the HEAT subroutine:

Card 6

1-80	Title	VKF Aerothermal Tunnel, Mach 4
------	-------	-----------------------------------

Card 7

1-80	MATL	Beryllium Copper 25
------	------	---------------------

Card 8

1-7	CD	507.5
8-14	DKDT	0.462
15-21	DM	0.25
22-28	DW	0.25
29-35	R4	20.0

Card 8

Columns	Input	Example Value
36-42	R5	20.0
43-49	GPM	200.0
50-56	ALPHA	9.6 E - 6
		(Exponent must be right-justified)
57-63	EMOD	30.0 E + 6
		(Exponent must be right-justified)
64-70	RNU	0.3
71-77	PW	70.0

Card 9

1-8	TN	30.0
9-16	RE	19.0
17-24	XC	7.0
25-28	NN	4.0
29-32	N	2.0

Card 10

1-8	DM	0.375
9-16	DW	0.25

Card 11

1-8	DM	0.3125
9-16	DW	0.25

Card 12

Columns	Input	Example Value
1-8	DM	0.3125
9-16	DW	0.25

Card 13

1-8	DM	0.375
9-16	DW	0.25

Computer Output--Example Problem

HEAT TRANSFER AND STRESS ANALYSIS SUMMARY
VKF AEROTHERMAL TUNNEL - MACH 4

DESIGN CONDITIONS

STAGNATION PRESSURE (PSI) = 211.00
 STAGNATION TEMPERATURE (DEG.H) = 1638.00
 COOLING WATER FLOW RATE (GPM) = 200.00
 COOLING WATER PRESSURE (PSI) = 70.00
 LINER MATERIAL-BERYLIUM COPPER 25

NOMENCLATURE FOR RESULTS

- X - LOCATION OF POINT BEING ANALYZED (IN.)
- R1 - INSIDE LINER RADIUS (IN.)
- R2 - OUTSIDE LINER RADIUS (IN.)
- R3 - INSIDE RADIUS OF COOLING WATER HOUSING (IN.)
- HA - LINER AIRSIDE HEAT TRANSFER COEFFICIENT (BTU/SEC/SQ.FT./DEG.F)
- HW - LINER WATERSIDE HEAT TRANSFER COEFFICIENT (BTU/SEC/SQ.FT./DEG.F)
- CD - LINER METAL CONDUCTIVITY (BTU-IN./HR/SQ.FT./DEG.F)
- TA - LINER AIRSIDE METAL TEMPERATURE (R)
- TW - LINER WATERSIDE METAL TEMPERATURE (R)
- TR - LINER AIRSIDE BOUNDARY LAYER RECOVERY TEMPERATURE (R)
- STHI - LINER AIRSIDE THERMAL CIRCUMFERENTIAL STRESS (PSI)
- STHO - LINER WATERSIDE THERMAL CIRCUMFERENTIAL STRESS (PSI)
- STAI - LINER AIRSIDE THERMAL AXIAL STRESS (PSI)
- STAO - LINER WATERSIDE THERMAL AXIAL STRESS (PSI)
- SAHI - LINER AIRSIDE AIR PRESSURE CIRCUMFERENTIAL STRESS (PSI)
- SAHO - LINER WATERSIDE AIR PRESSURE CIRCUMFERENTIAL STRESS (PSI)
- SAA - LINER AIR PRESSURE AXIAL STRESS (PSI)
- SWHI - LINER AIRSIDE WATER PRESSURE CIRCUMFERENTIAL STRESS (PSI)
- SWHO - LINER WATERSIDE WATER PRESSURE CIRCUMFERENTIAL STRESS (PSI)
- SWA - LINER WATER PRESSURE AXIAL STRESS (PSI)
- STYI - LINER AIRSIDE VON MISES-HENKY THEORY OF FAILURE YIELD STRESS (PSI)
- STYO - LINER WATERSIDE VON MISES-HENKY THEORY OF FAILURE YIELD STRESS (PSI)

LOCATION AND RADIUS:

X(IN)= 0.0
 R1(IN)= 19.0000
 R2(IN)= 19.3750
 R3(IN)= 19.6250

HEAT TRANSFER RESULTS:

HA(BTU/SEC/SQ.FT./DEG.F)= 0.0112
 HW(BTU/SEC/SQ.FT./DEG.F)= 0.1467
 CD(BTU-IN./HR/SQ.FT./DEG.F)= 789.7341
 TA(DEG.R)= 620.55
 TW(DEG.R)= 601.25
 TR(DEG.R)= 1637.98

STRESS RESULTS:

THERMAL---STHI(PSI)= -3997.
 STHO(PSI)= 3945.
 STAI(PSI)= -3997.
 STAO(PSI)= 3945.

PRESSURE--SAHI(PSI)= 10801.
 SAHO(PSI)= 10590.
 SAA(PSI)= -572.
 SWHI(PSI)= -3652.
 SWHO(PSI)= -3582.
 SWA(PSI)= 120.

VON MISES-HENCKY THEORY OF FAILURE

STYI(PSI)= 6597.
 STYU(PSI)= 9743.

* * * * *

LOCATION AND RADIUS: X (IN) = 23.0379
 R1 (IN) = 12.8324
 R2 (IN) = 13.1449
 R3 (IN) = 13.3949

HEAT TRANSFER RESULTS: HA (BTU/SEC/SQ.FT./DEG.F) = 0.0225
 HW (BTU/SEC/SQ.FT./DEG.F) = 0.2058
 CD (RTU-IN./HR/SQ.FT./DEG.F) = 805.2529
 TA (DEG.R) = 659.67
 TW (DEG.R) = 629.31
 TR (DEG.R) = 1637.90

STRESS RESULTS: THERMAL---STHI (PSI) = -6295.
 STHO (PSI) = 6195.
 STAI (PSI) = -6295.
 STAO (PSI) = 6195.

PRESSURE--SAHI (PSI) = 8780.
 SAHO (PSI) = 8569.
 SAA (PSI) = -6122.
 SWHI (PSI) = -2980.
 SWHO (PSI) = -2910.
 SWA (PSI) = 1959.

VON MISES-HENCKY THEORY OF FAILURE
 STYI (PSI) = 10108.
 STY0 (PSI) = 11024.

* * * * *

* * * * *

LOCATION AND RADIUS:	X(IN)=	46.0759
	R1(IN)=	3.7483
	R2(IN)=	3.9983
	R3(IN)=	4.2483

HEAT TRANSFER RESULTS:	HA(BTU/SEC/SQ.FT./DEG.F)=	0.1825
	HW(BTU/SEC/SQ.FT./DEG.F)=	0.5743
	CD(BTU-IN./HR/SQ.FT./DEG.F)=	881.3044
	TA(DEG.R)=	875.13
	TW(DEG.R)=	743.08
	TR(DEG.R)=	1607.36

STRESS RESULTS:	THERMAL---STHI(PHI)=	-27748.
	STHO(PHI)=	26579.
	STAI(PHI)=	-27748.
	STAO(PHI)=	26579.

	PRESSURE--SAHI(PHI)=	1635.
	SAHO(PHI)=	1529.
	SAA(PHI)=	-32593.
	SWHI(PHI)=	-1156.
	SWHO(PHI)=	-1086.
	SWA(PHI)=	13880.

VON MISES-HENCKY THEORY OF FAILURE

	STYI(PHI)=	40342.
	STYO(PHI)=	24124.

* * * * *

* * * * *

LOCATION AND RADIUS:	X (IN) =	49.9435
	R1 (IN) =	4.0305
	R2 (IN) =	4.3430
	R3 (IN) =	4.5930

HEAT TRANSFER RESULTS:	HA (BTU/SEC/SQ.FT./DEG.F) =	0.1418
	HW (BTU/SEC/SQ.FT./DEG.F) =	0.5270
	CD (RTU-IN./HR/SQ.FT./DEG.F) =	866.1103
	TA (DEG.R) =	842.03
	TW (DEG.R) =	710.39
	TR (DEG.R) =	1584.70

STRESS RESULTS:	THERMAL---STHI (PSI) =	-27754.
	STHO (PSI) =	26406.
	STAI (PSI) =	-27754.
	STAO (PSI) =	26406.

PRESSURE--SAHI (PSI) =	1088.
SAHO (PSI) =	1007.
SAA (PSI) =	-24054.
SWHI (PSI) =	-1009.
SWHO (PSI) =	-939.
SWA (PSI) =	10196.

VON MISES-HENCKY THEORY OF FAILURE	
STYI (PSI) =	36610.
STY0 (PSI) =	22997.

* * * * *

* * * * *

LOCATION AND RADIUS:

X(IN) = 60.0000
 R1(IN) = 5.5202
 R2(IN) = 5.8952
 R3(IN) = 6.1452

HEAT TRANSFER RESULTS:

HA(BTU/SEC/SQ.FT./DEG.F) = 0.0669
 HW(BTU/SEC/SQ.FT./DEG.F) = 0.3965
 CD(BTU-IN./HR/SQ.FT./DEG.F) = 829.0380
 TA(DEG.R) = 738.73
 TW(DEG.R) = 653.22
 TR(DEG.R) = 1550.87

STRESS RESULTS:

THERMAL---STHI(PSI) = -17977.
 STHO(PSI) = 17206.
 STAI(PSI) = -17977.
 STAO(PSI) = 17206.
 PRESSURE--SAHI(PSI) = 934.
 SAHO(PSI) = 873.
 SAA(PSI) = -14510.
 SWHI(PSI) = -1137.
 SWHO(PSI) = -1067.
 SWA(PSI) = 5973.

VON MISES-HENCKY THEORY OF FAILURE

STYI(PSI) = 23425.
 STYO(PSI) = 14795.

* * * * *

The sample problem results are plotted on Fig. 4. The liner radial thermal gradient and thermal stresses become a maximum near the throat. The calculated yield stress is also maximum near the throat, indicating its dependence on thermal stress. The pressure stresses generally become a minimum at the throat.

The maximum calculated yield stress was 40 ksi at the throat. The yield strength of the candidate material, BeCu 25, at a temperature of (T_a) 875°R, was 140 ksi. Thus, the safety factor was 140/40 or 3.5. A safety factor of two is considered to be the allowable minimum.

The other primary point to consider is the saturation pressure of water at the waterside liner metal temperature, T_w . This temperature was 743°R, and the saturation pressure from a standard steam table was 52 psia. The cooling-water supply pressure was 70 psia, and even though some losses are expected, the safety factor of 1.35 should be adequate.

The liner end support calculations would next be made to complete analysis of this candidate material.

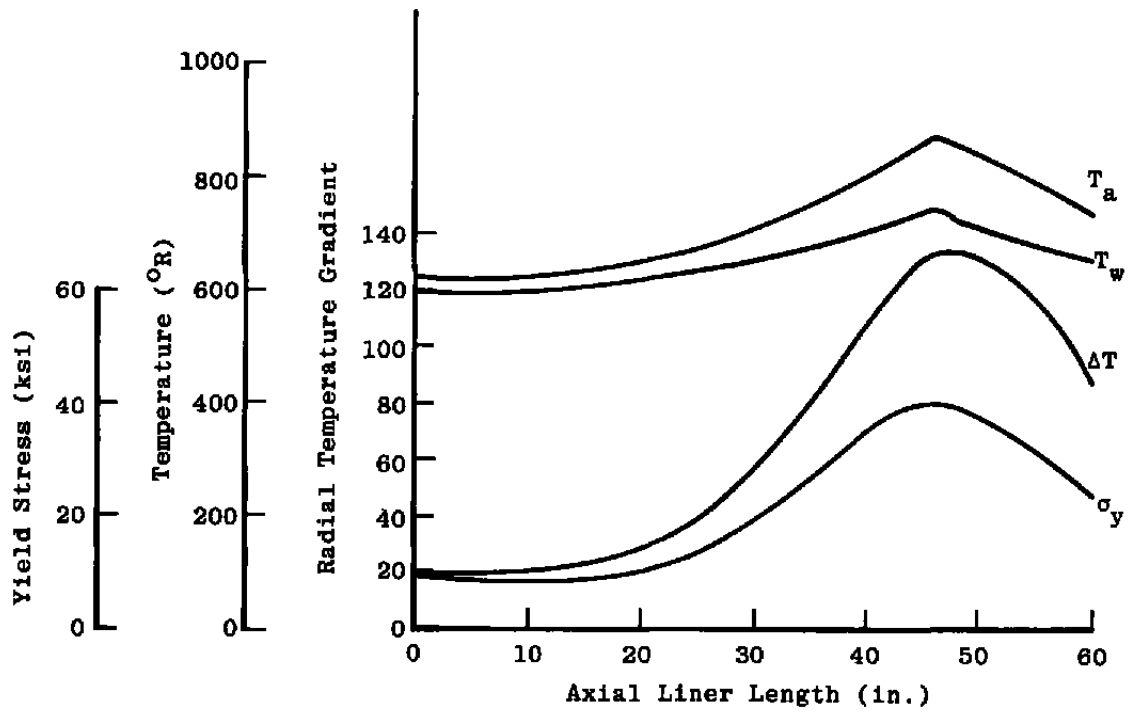


Figure 4. Example problem results.

BIBLIOGRAPHY

1. Sivells, James C. "Aerodynamic Design of Axisymmetric Hypersonic Wind-Tunnel Nozzles." American Institute of Aeronautics and Astronautics Paper No. 69-337, presented at AIAA 4th Aerodynamic Testing Conference, Cincinnati, Ohio, April 28-30, 1969.
2. Sivells, James C. "A Computer Program for the Aerodynamic Design of Axisymmetric and Planar Nozzles for Supersonic and Hypersonic Wind Tunnels." Unpublished technical report, Arnold Engineering Development Center, Arnold Air Force Station, Tennessee, 1978.
3. Sivells, James C. "Aerodynamic Design and Calibration of the VKF 50-Inch Hypersonic Wind Tunnel," Arnold Engineering Development Center TDR-62-230, Arnold Air Force Station, Tennessee, March, 1963.
4. Bartz, D. R. "A Simple Equation for Rapid Estimation of Rocket Nozzle Convective Heat Transfer Coefficients," Jet Propulsion Journal of the American Rocket Society, 27:49-51, January, 1957.
5. Bartz, D. R. "An Approximate Solution of Compressible Turbulent Boundary-Layer Development and Convective Heat Transfer in Convergent-Divergent Nozzles." American Society of Mechanical Engineers Paper No. 54-A-153, presented at the ASME Annual Meeting, New York, New York, November 28-December 3, 1954.
6. Holman, J. P. Heat Transfer. First edition. New York: McGraw-Hill Book Company, Inc., 1963.
7. Eckert, Ernst R. G. "Survey on Heat Transfer at High Speeds," Wright Air Development Center TR-54-70, Wright-Patterson Air Force Base, Ohio, April, 1954.
8. van Driest, E. R. "The Problem of Aerodynamic Heating," Aeronautical Engineering Review, 15(No. 10):26-41, October, 1956.
9. Ames Research Staff. "Equations, Tables, and Charts for Compressible Flow," National Advisory Committee for Aeronautics Report 1135, Ames Aeronautical Laboratory, Moffett Field, California, 1953.

10. Dorn, W. S., and D. D. McCracken. Numerical Methods with Fortran IV Case Studies. First edition. New York: John Wiley and Sons, Inc., 1972.
11. Brown, A. I., and S. M. Marco. Introduction to Heat Transfer. Third edition. New York: McGraw-Hill Book Company, Inc., 1958.
12. Back, L. H., P. F. Massier, and R. F. Cuffel. "Flow and Heat-Transfer Measurements in Subsonic Air Flow through a Contraction Section," International Journal of Heat Mass Transfer, 12:1-13, 1969.
13. Timoshenko, S. P., and J. N. Goodier. Theory of Elasticity. Third edition. New York: McGraw-Hill Book Company, Inc., 1970.
14. Shigley, J. E. Engineering Design. First edition. New York: McGraw-Hill Book Company, Inc., 1963.

APPENDIX A EQUATION DEVELOPMENT FOR SMOOTH SUBSONIC CONTOURS

Many aerodynamicists believe that airflow properties in supersonic nozzles are much more uniform if a smooth, continuous contour is a design factor. Thus, in design of liners at the VKF of AEDC the following theory has been used (see Fig. 5).

A fourth-order polynomial equation defines the contour from the entrance to the conical section. A third-, or fourth-order, polynomial equation defines the contour from the cone to the throat.

To have a smooth contour, there must be no discontinuities when changing from one shape to the next. This dictates the boundary conditions to establish the curves that define the contour.

Starting at the throat and working upstream, one can easily develop the appropriate constants for the polynomial equations that define the contour. The known values are the throat radius, R_S ; radius of curvature at the throat, R^* ; the total length of the throat, X_L ; the slope of the conical section, T_N ; and the entrance radius to the liner, R_E . From these known values and the boundary conditions the contour equations can be derived.

If a third-order equation is chosen for the entrance to the throat, a common form is

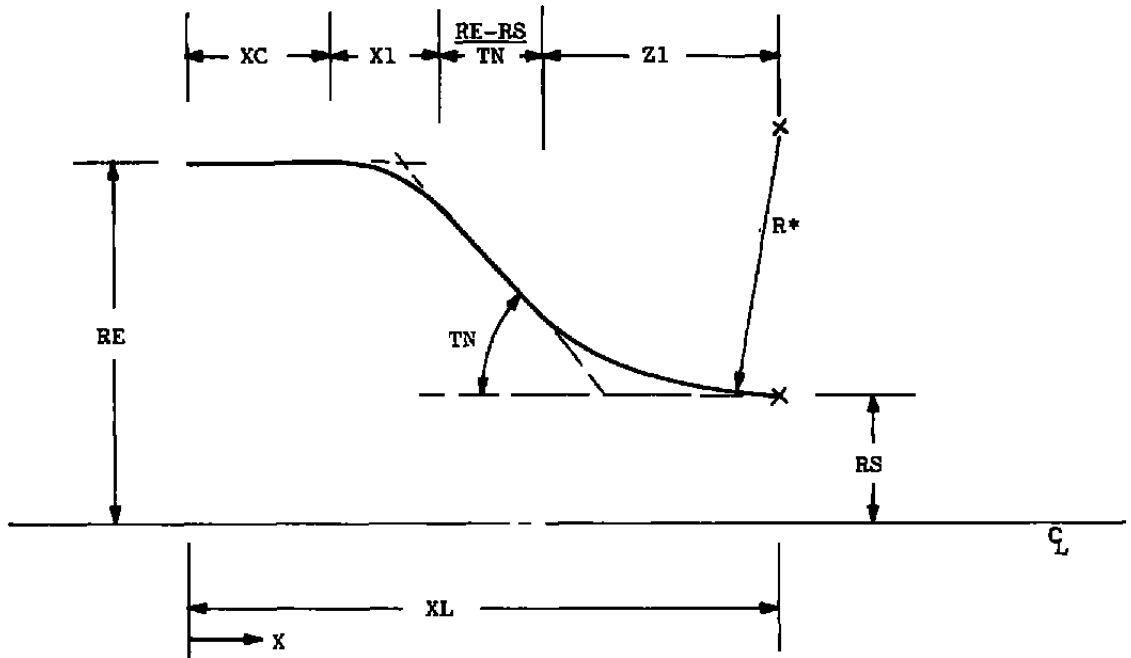


Figure 5. Continuous smooth curvature for liner subsonic section.

$$R = A + B \left(\frac{X_L - X}{Z_1} \right)^2 + C \left(\frac{X_L - X}{Z_1} \right)^3 . \quad (A-1)$$

The variable was nondimensionalized for simpler calculations. At the throat the boundary condition of known radius of curvature is used. Let

$$Z_R = \frac{X_L - X}{Z_1}$$

and Eq. (A-1) then becomes

$$R = A + B (Z_R)^2 + C (Z_R)^3 . \quad (A-2)$$

The first derivative of R with respect to ZR is

$$\frac{dR}{d(ZR)} = 2B (Z_R) + 3C (Z_R)^2 . \quad (A-3)$$

The second derivative is

$$\frac{d^2R}{d(ZR)^2} = 2B + 6C (Z_R) . \quad (A-4)$$

From the boundary conditions,

$$\frac{d^2R}{dX^2} = \frac{1}{R^*} \quad (A-5)$$

at $X = X_L$ or $Z_R = 0$.

The equation for R is a function of ZR, not X; therefore, the chain rule of differentiation must be used. The differentiated equation is

$$\frac{dR}{dX} = \left[\frac{dR}{d(ZR)} \right] \left[\frac{d(ZR)}{dX} \right] , \quad (A-6)$$

which is the slope. The curvature equation is

$$\frac{d^2R}{dX^2} = \left[\frac{d^2R}{d(ZR)^2} \right] \left[\frac{d(ZR)}{dX} \right]^2 + \left[\frac{dR}{d(ZR)} \right] \left[\frac{d^2(ZR)}{dX^2} \right] . \quad (A-7)$$

Now the derivatives of ZR with respect to X must be found.

They are

$$\frac{d(ZR)}{dX} = \frac{d \left(\frac{XL - X}{Z1} \right)}{dX} = - \frac{1}{Z1} \quad (A-8)$$

and

$$\frac{d^2(ZR)}{dX^2} = 0 . \quad (A-9)$$

The resulting equation for one of the polynomial constants using the boundary condition, Eq. (A-5), and Eqs. (A-4), (A-7), (A-8), and (A-9) is

$$\frac{1}{R^*} = 2B \left(- \frac{1}{Z1} \right)^2 .$$

The equation for B is

$$B = \frac{(Z1)^2}{2R^*} . \quad (A-10)$$

An equation for A can be found from the boundary condition that $R = RS$ at $X = XL$, ($ZR = 0$) and the polynomial equation, Eq. (A-1). The equation is

$$RS = A . \quad (A-11)$$

Other boundary conditions to be used are the slope and curvature at $X = XL - X1$, ($ZR = 1$) and must be equal to $-TN$ and 0 , respectively. Thus, $Z1$ and the other polynomial constant, C , can be found from these boundary conditions and Eqs. (A-3), (A-4), (A-6), (A-7), (A-8), and (A-9). The constant, C , is

$$\frac{dR}{dX} = -TN = \left(-\frac{1}{Z1}\right) (2B + 3C)$$

or

$$(TN)(Z1) = 2B + 3C . \quad (A-12)$$

The value of B is already known from Eq. (A-10); therefore,

$$(TN)(Z1) = \frac{Z1^2}{R^*} + 3C$$

and

$$C = \frac{(TN)(Z1)}{3} - \frac{Z1^2}{3R^*} . \quad (A-13)$$

The equation of Z1 is found by using the curvature boundary condition, Eq. (A-5), with Eqs. (A-7) through (A-10), and (A-13). The results are

$$\frac{d^2R}{dX^2} = 0 = (2B + 6C) \left(-\frac{1}{Z1}\right)^2,$$

or, simplifying,

$$B = 3C$$

and

(A-14)

$$Z1 = 2R^*(TN) .$$

Now, the third-order polynomial equation can be found by substituting Eqs. (A-10), (A-11), and (A-13) into (A-2) and simplifying. The result is

$$R = RS + 2R^*(TN)^2 (ZR)^2 - \frac{2}{3} R^*(TN)^2 (ZR)^3 . \quad (A-15)$$

If a fourth-order equation is desired for the throat region, the same procedure is followed as for the third-order, except the initial Eq. (A-2) is changed to

$$R = A + B (ZR)^2 + C (ZR)^4 . \quad (A-16)$$

Since the derivation is identical to the third-order equation, only the results are shown.

The length of the fourth-order contour at the throat is

$$Z_1 = (3/2) (R^*) (TN) . \quad (A-17)$$

The fourth-order equation that describes the contour is

$$R = RS + (9/8) (TN)^2 (R^*) (ZR)^2 - (3/16) (TN)^2 (R^*) (ZR)^4 . \quad (A-18)$$

The length of the curved section near the throat was evaluated in Eqs. (A-14) and (A-17) for a third- and fourth-order contour, respectively. The intercept of the cone contour with a line parallel to the centerline and running through the throat radius, RS , is helpful in defining the conical contour equation. The fractional length of Z_1 can be used to define that dimension.

For the third-order curve, Fig. 5, page 65, the radius at $X = (XL - Z_1)$, ($ZR = 1$), is defined by Eq. (A-15). The resulting equation is

$$R = RS + (4/3) (R^*) (TN)^2 . \quad (A-19)$$

Thus, the fractional length $(1 - \alpha) Z_1$ can be determined by trigonometry, and is

$$TN = \frac{R - RS}{(1 - \alpha) (Z_1)} . \quad (A-20)$$

If Eqs. (A-14) and (A-19) are substituted into (A-20), it can be shown that

$$\alpha = 1/3 \quad (\text{A-21})$$

for the cubic contour curve. The same derivation for the fourth-order curve results in the following equations:

$$R = RS + (15/16)(R^*)(TN)^2 \quad (\text{A-22})$$

at

$$X = XL - Z1, \quad ZR = 1,$$

and

$$\alpha = 3/8. \quad (\text{A-23})$$

Now, the conical contour equation can be determined from Fig. 5, page 65,

$$R = RE + \left(\frac{X1}{2}\right)(TN) - (TN)(X - XC). \quad (\text{A-24})$$

The length, $X1$, of the fourth-degree entrance curve can be found from Fig. 5. The equation is

$$XL = XC + \frac{X1}{2} + \frac{RE - RS}{TN} + \alpha(Z1)$$

or

$$\frac{X1}{2} = XL - XC - \left(\frac{RE - RS}{TN}\right) - \alpha(Z1). \quad (\text{A-25})$$

Equations (A-21) and (A-23) define α . Thus, for a third-order contour near the throat, the length, $X1$, of the

entrance fourth-order curve is

$$X1 = 2 \left(XL - XC - \left(\frac{RE - RS}{TN} \right) - (1/3) Z1 \right) . \quad (A-26)$$

For a fourth-order contour near the throat the length of the entrance fourth-order contour is

$$X1 = 2 \left(XL - XC - \left(\frac{RE - RS}{TN} \right) - (3/8) Z1 \right) . \quad (A-27)$$

The entrance contour is usually a fourth-order polynomial of the form

$$R = A + B (XR)^3 + C (XR)^4 , \quad (A-28)$$

where XR is a nondimensionalized variable defined as

$$XR = \frac{X - XC}{X1} . \quad (A-29)$$

Following the same procedure as for the polynomials at the throat entrance, one can derive the fourth-order contour equation. The boundary conditions are

$$R = RE \text{ at } X = XC, (XR = 0) , \quad (A-30)$$

and the slope and curvature are equal to

$$\frac{dR}{dX} = - TN \quad (A-31)$$

and

$$\frac{d^2R}{dX^2} = 0 , \quad (A-32)$$

respectively, at

$$X = X_C + X_1, \quad (X_R = 1) .$$

The derivatives of Eq. (A-28) required for solution are

$$\frac{dR}{d(XR)} = 3B (XR)^2 + 4C (XR)^3 \quad (A-33)$$

and

$$\frac{d^2R}{d(XR)^2} = 6B (XR) + 12C (XR)^2 , \quad (A-34)$$

where the relation between $R(X)$ and $R(XR)$ is

$$\frac{dR}{dX} = \left[\frac{dR}{d(XR)} \right] \left[\frac{d(XR)}{dX} \right] \quad (A-35)$$

and

$$\frac{d^2R}{dX^2} = \left[\frac{d^2R}{d(XR)^2} \right] \left[\frac{d(XR)}{dX} \right]^2 + \left[\frac{dR}{d(XR)} \right] \left[\frac{d^2(XR)}{dX^2} \right] . \quad (A-36)$$

The derivatives of $XR(X)$ from Eq. (A-29) are

$$\frac{d(XR)}{dX} = \frac{1}{X_1} \quad (A-37)$$

and

$$\frac{d^2(XR)}{dX^2} = 0 . \quad (A-38)$$

The constant, A, can be found from Eqs. (A-28) and (A-30).

The equation for A is

$$RE = A . \quad (A-39)$$

The equations for constants B and C are then found from boundary condition equations, Eqs. (A-31) and (A-32), and relation equations, Eqs. (A-33) through (A-38). The intermediate equations are

$$-TN = (3B + 4C) \left(\frac{1}{X1} \right) , \quad (A-40)$$

and

$$\left. \begin{aligned} 0 &= (6B + 12C) \left(\frac{1}{X1} \right)^2 \\ B &= -2C . \end{aligned} \right\} \quad (A-41)$$

Substitution of Eq. (A-41) into (A-40) yields the equation for C:

$$\begin{aligned} (-X1)(TN) &= -6C + 4C \\ C &= \frac{(TN)(X1)}{2} . \end{aligned} \quad (A-42)$$

The final equation for B is found by substituting Eq. (A-42) into (A-41):

$$B = -(TN)(X1) . \quad (A-43)$$

Thus, the fourth-order contour equation for the entrance to the liner is found by substituting Eqs. (A-39), (A-42), and

(A-43) into (A-28). The result is

$$R = RE - (TN)(X1)(XR)^3 + \frac{(TN)(X1)}{2} (XR)^4 . \quad (A-44)$$

All of the contour equations have been programmed using the same nomenclature in which they were derived in this appendix. The polynomials used in this derivation are typical for liners at the VKF of AEDC.

APPENDIX B AXIAL FORCE EQUATION DEVELOPMENT

Subsonic Section

Most liners in current use at the VKF of AEDC are fixed on the supersonic end, and the subsonic end is free to move to eliminate stresses due to restrained thermal expansion. Therefore, any axial pressure loads on the liner are transferred through the liner to the fixed end (see Fig. 1, page 3). Figures 6 and 7 illustrate how the liner segments are loaded.

The air pressure in the liner varies along its entire length. The pressure is a maximum at the upstream subsonic end and a minimum at the downstream supersonic end. The variation is given by Eq. (7):

$$P_{\infty} = P_0 \left[1 + \left(\frac{\gamma-1}{2} \right) M^2 \right]^{-\frac{\gamma}{\gamma-1}} \quad (B-1)$$

In this equation, P_0 is the stagnation pressure for the tunnel, and γ is the specific heat ratio for air. The Mach number, M , is calculated by the heat-transfer analysis described in Chapters II and III.

The procedure used for calculating the axial force at any location along the liner was as follows. First, the force caused by the air pressure acting on the area between

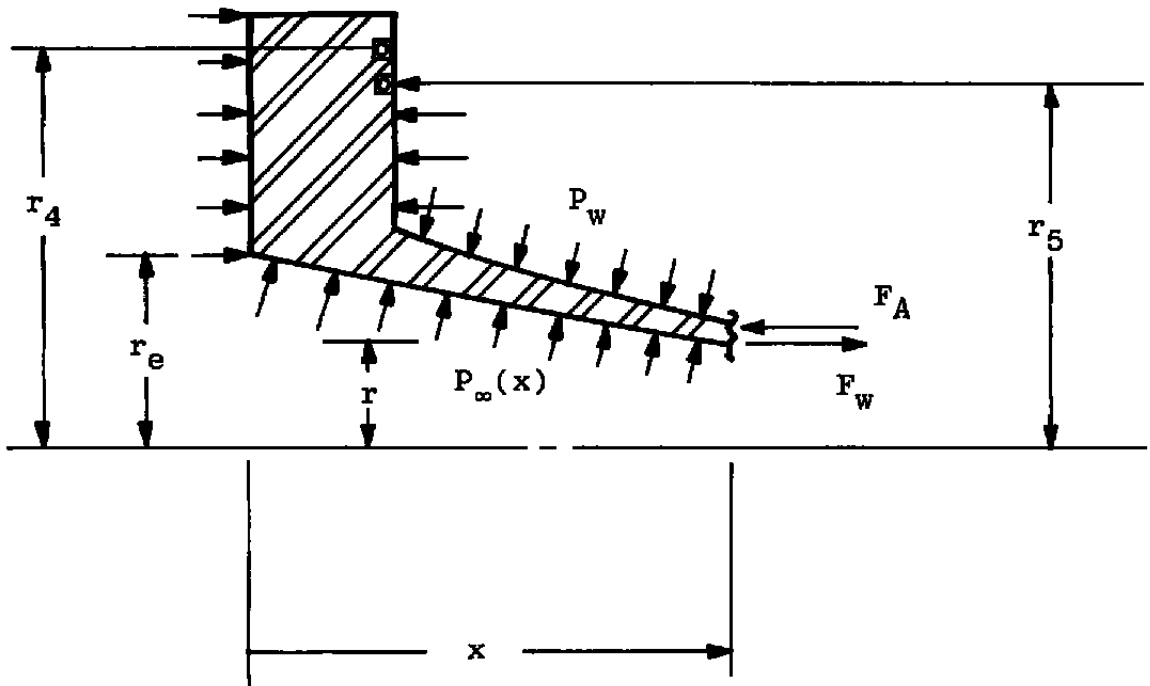


Figure 6. Liner segment showing load distribution for subsonic section.

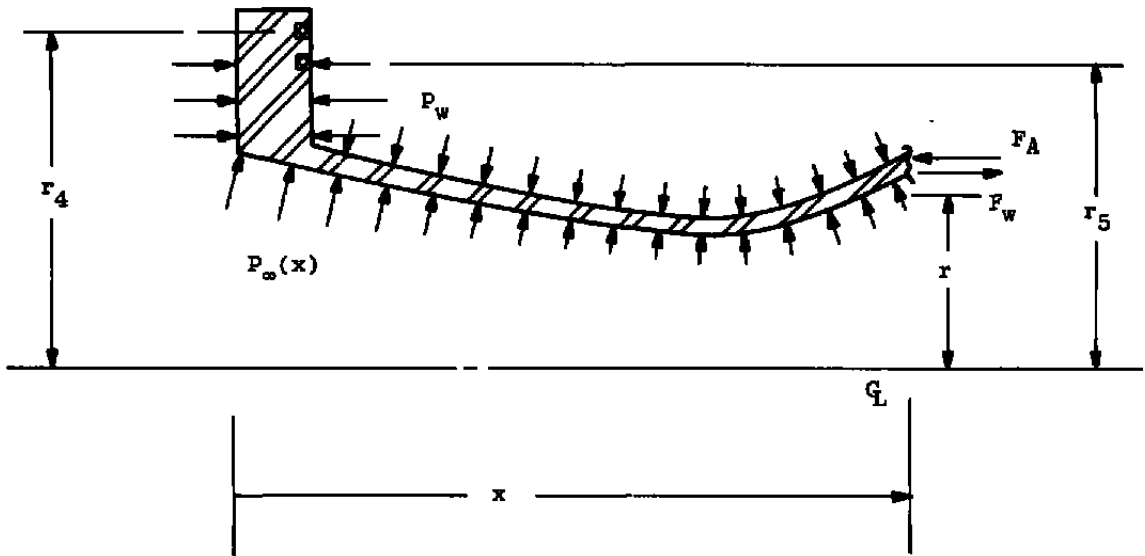


Figure 7. Liner segment showing load distribution for supersonic section.

the seal radius, r_4 , and the entrance radius, r_e , was determined (see Fig. 6). Secondly, the average air pressure between the entrance and the location of interest was determined. This average pressure was multiplied by the projected area between the entrance to the liner and the location of interest to obtain an axial force. The total axial force was obtained by adding the above two force components. In equation form, the axial force is given by

$$F_a = \pi (r_e^2 - r_l^2) P_m + P_e \pi (r_4^2 - r_e^2), \quad (B-2)$$

where

$$P_m = \frac{P_e + P_\infty}{2}. \quad (B-3)$$

Obviously, the calculations could be made more exact by dividing the liner into short sections, calculating the force on each, and adding all of the forces for the total. The axial pressure stresses are generally small in comparison to the thermal ones; therefore, the extra effort was not warranted.

It was assumed that the cooling-water pressure drop as it flows through the liner was not significant enough to require the pressure-averaging technique. Therefore, the water pressure was multiplied times the appropriate projected area to obtain the axial force due to water

pressure. The equation is

$$F_w = \pi (r_5^2 - r_2^2) P_w . \quad (B-4)$$

Supersonic Section

The axial loads for the supersonic liner section are shown on Fig. 7. Note that the air-pressure load on the supersonic side subtracts from the air-pressure load on the subsonic side. The water-pressure loads in the two liner sections oppose too; hence, the total load calculated for the throat section for both water and air is the maximum load that the liner sees. The load equations are

$$F_a = \pi (r_4^2 - r_e^2) P_e + \pi (r_e^2 - r_1^{*2}) P_{m,b} - \pi (r_1^2 - r_1^{*2}) P_{m,p} , \quad (B-5)$$

where

$$P_{m,b} = \frac{P_\infty^* + P_e}{2} \quad (B-6)$$

and

$$P_{m,p} = \frac{P_e + P_\infty}{2} . \quad (B-7)$$

The total force equation due to water pressure remains the same, Eq. (B-4).

NOMENCLATURE

A	Area, constant, reference point
B	Constant, reference point
C	Constant, reference point
C _p	Specific heat
C _f	Skin-friction coefficient
C*	Characteristic velocity
C	Circumference
D	Hydraulic diameter
d	Diameter
E	Modulus of elasticity, reference point
F	Force
G	Mass velocity
g	Gravitational acceleration
h	Heat-transfer coefficient
I	Reference point
K	Metal conductivity
k	Gas conductivity
L	Length
ΔL	Incremental length
M	Mach number
P	Pressure, perimeter
P _c	Peclet number
Pr	Prandtl number
q	Heat-transfer rate

R	Gas constant, radius
RE	Subsonic section entrance radius
RS	Radius at the throat
Re	Reynolds number
R*	Radius of curvature at throat
r	Radius, recovery factor
Δr	Incremental radius
St	Stanton number
T	Temperature, reference point
Tb	Bulk temperature
Tr	Recovery temperature
TN	Tangent of angle between conical section and liner axis in subsonic section
TP	Reference temperature
ΔT	Temperature difference
t	Liner thickness
tw	Water-passage thickness
u	Velocity
X	Variable
XC	Length of constant diameter entrance to subsonic section
XL	Subsonic liner length
X1	Length of subsonic liner segment between entrance and conical section
x	Distance
ZR	Variable

Z1 Length of subsonic liner segment between throat and conical section

Greek Letters

α Coefficient of expansion, constant
 γ Specific heat ratio
 θ Cone angle
 μ Poisson ratio, viscosity
 ρ Density
 ρ_c Modified density
 σ Variable, stress

Subscripts

A Axial
a Airside
b Subsonic
c Critical
e Entry
i Inside
K Conductivity
m Mean value
o Stagnation
p Supersonic
r Radial
s Speed of sound
w Waterside
y Yield

- z Axial
- θ Circumferential
- ∞ Static
- 1 Inside of liner
- 2 Outside of liner
- 3 Outside of water channel
- 4 Air seal
- 5 Water seal

Superscript

- * Throat